TÉCNICO LISBOA

Modelling Phase Equilibria, Transport and Interfacial Properties of Mixtures of Fluorinated and Hydrogenated Alcohols

João Eduardo Duarte

Thesis to obtain the Master of Science Degree in

Chemical Engineering

Supervisors:

Dr. Eduardo Filipe

Dr. Lourdes F. Vega

Examination Committee

Chairperson: Dr. Sebastião Alves

Supervisor: Dr. Eduardo Filipe

Members of the Committee: Dr. Luís Filipe Martins

October 2019

Acknowledgments

The achievement of this thesis brought me so good things to my path, and for that reason, I like to thank the opportunity and support given me by some people.

I want to thank my supervisor Professor Eduardo Filipe that allowed me to do this thesis in the first place. I will never forget the passion and the clarity given about the work done by the group. His support and teachings throughout the entire journey were spotless.

I would like to acknowledge my other supervisor Professor Lourdes Vega that grants me the opportunity to work with her in Abu Dhabi and teaching me so many things and not only about the work. It is impossible to thank all the hours and work given for my stay in Abu Dhabi, and I will never forget her hospitality. Without the help of her and the group my stay in Abu Dhabi, it would have been entirely different, so I am thankful for their friendship. Moreover, I particularly like to thank Ismail Alkhatib that was always willing to help me.

I could not ask for better supervisors, and they will always be an example of life and success.

I also want to thank Khalifa University for the financial support that allowed my stay in Abu Dhabi through project GRC2018-003.

Finally, I need to thank my family and friends that gave me all the support that I needed on this journey. Each of them enabled me to have one of the best moments of my life, and I will forever be grateful.

“Writing is good; thinking is better. Cleverness is good; patience is better.”
— Hermann Hesse, Siddhartha

Abstract

In this dissertation, soft-SAFT jointed with the Free-Volume Theory (FTV), is used to describe the viscosities of the pure fluorinated alcohols and the mixtures between fluorinated and hydrogenated alcohols. The fitting of the parameters to describe the pure viscosities was completed in association with the viscosities of the mixtures by a methodology called Spider-Web, achieving a robust model with accurate results.

The fluorinated and hydrogenated alcohols mixtures have unique and exciting properties, mostly, at the interface were a minimum called aneotrope appears in the surface tension over the composition. To improve the knowledge about these mixtures first is crucial to study the fluorinated and hydrogenated mixtures (without the OH group). By analyzing the Hexane and Perfluorohexane mixture and transferring the adjustable parameters fitted for this mixture to the fluorinated and hydrogenated alcohols mixtures made possible deep and more rebuts results. The results from the model and by only adjust the association for the fluorinated and hydrogenated alcohols mixtures shows good agreement when compared to the experimental and simulation data available in the literature.

The description of surface tensions of the mixtures using soft-SAFT coupled with the Density Gradient Theory (DGT) is achieved showing good agreement with the experimental data available in the literature, and with success captured the aneotrope. In order to have a deeper appreciation of the surface tensions and the phenomena's that occur at the interface, the microscopic structure was also studied by analyzing the Adsorptions and Density Profiles.

Keywords: soft-SAFT, Fluorinated Alcohols, Viscosity, FTV, Interface Properties, DGT.

Resumo

Nesta dissertação soft-SAFT em conjunto com a teoria do volume livre FTV, são usadas para descrever as viscosidades dos álcoois fluorados puros e das misturas entre os álcoois fluorados e hidrogenados. A parametrização para descrever as viscosidades dos puros foi feita associando também os dados experimentais das misturas, através de uma metodologia chamada Spider-Wed, atingindo um modelo robusto com resultados precisos.

As misturas entre álcoois fluorados e hidrogenados têm propriedades atípicas e estimulantes, principalmente, à superfície onde um mínimo denominado aneótropo aparece nas tensões superficiais em função da composição. Para melhorar o conhecimento acerca destas misturas é crucial primeiro estudar o que acontece nas misturas entre fluorados e hidrogenados (sem o grupo OH). Analisando a mistura entre Hexano e Perfluorohexano e transferindo os parâmetros de ajuste utilizados nesta mistura para as misturas entre álcoois fluorados e hidrogenados tronou possivel a obtenção de resultados mais fortes e robustos. Os resultados do modelo e apenas ajustando a associação para as misturas de álcoois fluorados com hidrogenados mostram uma boa concordância quando comparados com os resultados experimentais e de simulação que se encontram na literatura.

A descrição das tensões superficiais das misturas utilizando a soft-SAFT acoplada com a teoria de interfaces DGT foi atingida, mostrando uma boa concordância com os dados experimentais disponíveis na literatura, e o aneótropo foi capturado com sucesso. De modo a ter um conhecimento mais profundo acerca das tensões superficiais e dos fenómenos que ocorrem na superfície foi também estuda a estrutura microscópica analisando as adsorções e os perfis de densidade.

Palavras-chave: soft-SAFT, Álcoois Fluorados, Viscosidade, FTV, Propriedades da Interface, DGT.

Contents

List of Tables

List of figures

Nomenclature

Symbols

A^{res}	-	Residual Helmholtz free energy
A^{ref}	-	Reference term
A^{chain}	-	Chain term
A^{assoc}	-	Association term
N_m	-	Number of chain molecules
k_B	-	Boltzmann constant
T	-	Temperature
A^{ideal}	-	Ideal term
n_T	-	Number of components
i and ii	-	Component
x	-	Molar fraction
ρ_m	-	Molecular density
Λ	-	Thermal de Broglie wavelength
V	-	Volume
ϕ	-	Potential energy
r	-	Distance between two spheres
ε^{LJ}	-	LJ well depth
σ^{LJ}	-	LJ atomic diameter
m	-	Chain length
y_R	-	Contact value of the cavity correlation function for spherical segments
g_R	-	The prior radial distribution function of the LJ fluid
$\Gamma^{(i)}$	-	Sites of each species
X_A	-	The fraction of nonbonded sites A
Δ_{AB}	-	Association bond stretch between two sites
ε^{HB}	-	Energy of association
κ^{HB}	-	Association volume
σ	-	Crossed size parameter
ε	-	Energy parameter
$\eta_{ij}, \xi_{ij}, \alpha_{ij}^{HB}$ and β	-	Binary parameters
P	-	Pressure
μ	-	Chemical potential
ρ	-	Density

n	-	Mole fraction
ϕ_p	-	Fugacity coefficient
Υ	-	Activity coefficient
C_v	-	Isochoric heat capacity
k_T	-	Reduced bulk modulus
μ_{JT}	-	Joule-Thomson coefficient
α_E	-	Thermal expansion coefficient
C_p	-	Isobaric heat capacity
c	-	Speed of sound
γ	-	Surface tension
l	-	Length
A	-	Surface area
G	-	Gibbs free energy
S	-	Entropy
W	-	Work
Γ	-	Adsorption
z	-	The direction perpendicular to the interface
Δz	-	Thickness
$\tilde{a}$	-	Helmholtz free energy density
$\tilde{\rho}$	-	Local density
∇	-	Gradient
C	-	Influence parameter
t	-	Time
ν	-	Velocity
η	-	Dynamic viscosity
υ	-	Kinematic viscosity
$\Delta\eta$	-	Dense correction term
M_W	-	Molecular weight
v_c	-	Critical volume
Ω^*	-	Deduced collision integral for the LJ potential
F_c	-	Correction empirical factor
T_r	-	Reduced temperature
ω	-	Acentric factor
μ_r	-	Reduced dipole moment
k	-	Empirical parameter
N_A	-	Avogadro's number
ζ_0	-	Friction coefficient

L^2	-	Average quadratic length
B	-	Parameter related to the free-volume overlap
f_v	-	Free-volume fraction
R	-	Universal constant for gases
E	-	The potential energy of interaction
α	-	Activation energy parameter

Acronyms

EoS	-	Equations of State
SAFT	-	Statistical Associating Fluid Theory
C	-	Carbon
F	-	Fluor
O	-	Oxygen
H	-	Hydrogen
TFE	-	Trifluoroethanol
PFP	-	Pentafluoropropanol
HFB	-	Heptafluorobutanol
NFP	-	Nonafluoropentanol
UFH	-	Undecafluorohexanol
TRFH	-	Tridecafluoroheptanol
PDFO	-	Pentadecafluorooctanol
HS	-	Hard spheres
SW	-	Square well
LJ	-	Lennard-Jones
VLE	-	Vapor-Liquid Equilibrium
G	-	Gaseous phase
L	-	Liquid phase
DGT	-	Density Gradient Theory
FTV	-	Free-Volume Theory

1. Introduction

Knowing the thermodynamic properties of pure compounds and mixtures are essential to any chemical process. For that reason, having models that can predict, with accuracy, these properties are crucial to the industry. An accurate model can give property data that, in another way, is not founded. For instance, to predict properties that are difficult to obtain experimentally or in cases that the experimental research is expensive or requires substantial time.

There are two kinds of approaches to calculate these properties, besides the experimental, molecular simulations and theoretical models. There are many types of models used to calculate thermodynamic properties, such as Equations of State (EoS). An EoS is a thermodynamic equation that describes the state of matter using the relation between functions of state, like temperature and pressure. Many of these equations cannot describe the intermolecular interactions and the impact of the chemical structure of the molecule to obtain an accurate result. However, Statistical Associating Fluid Theory (SAFT) [1][2][3], have a different approach to this problem. This equation is a molecular-based model that accounts for the impact of the chemical structure and functional groups by explicitly taking them into account in the construction of the equation. For this reason, this equation can use in his model attractive highly directional forces like hydrogen bonding, one of the forces that have a powerful impact on a non-ideal model.

The recent increase of the fluorinated compounds and their mixtures in industrial applications comes from all the physical, chemical, and thermodynamic properties that these compounds have. Some of these applications are in refrigerants, batteries, firefighting foams, polymers, pharmaceutical reactants, as materials and biologically active agents, in medical chemistry, and much more.

Fluorine is one of the most electronegative elements that create powerful bonds, especially with carbon because of the high polarity created between the two components. Replacing the hydrogen atoms in an organic structure with fluorine is relatively simple because of the small atomic radius. This phenomenon has a substantial impact on the stability, biological availability, and activity of the molecule. The fluorine is also one of the most chemically reactive elements, and because of that, any reaction containing this substance requires specialized equipment and techniques.

Mixtures between fluorinated and hydrogenated compounds, as known, have a significant phase separation, which results in large positive excess properties and positive deviation to Raoult's law [4]. The interpretation of this behavior is due to the weak dispersion forces caused by the weak cross-interaction between the two different chains. Another fact is that the fluorinated chains are very rigid, and the hydrogenated flexible and the conflict of the cross-sectional diameters of the two different chains contribute to the segregation.

The fluorinated compound that this work is devoted to are the fluorinated alcohols, also known as fluorinated surfactants, with the general formula of $CF_3(CF_2)_n(CF_2)_m\ (1 \leq m \leq 2)$. These compounds have the hydrophilic and hydrophobic behavior, that come from the presence of a fluorinated chain, that intensify the hydrophobicity compared to the hydrogenated chain (this is due to the lower translational and rotational movement of the molecules), and a poorly understood antipathy relatively to common hydrogenated solvents. These molecules also have a higher dipole because of the electronegativity difference between the different sites of the molecule pulling the electronic cloud to the fluorine telomer side, turning the OH group more acid [5].

Because of the importance of these compounds is necessary to study the behavior, not only of the pure compound but also the mixtures. Furthermore, in this work, the focus is on fluorinated and hydrogenated alcohols mixtures. The two compounds are phobic, and the addition of an alcoholic polar group to the chains brings impressive thermodynamic results due to the existence of associative interactions between the two phobic sides of the molecules. Morgado [6] suggested that this chain will try to create an O···HO network of hydrogen bonds, surrounded by carbon chains tails, segregating into hydrogenated and fluorinated domains, achieving the best packing possible for the phobic sides. Because of the unique behavior between these two components at the interface, the two components interact in a certain way that a minimum in the surface tension over the compositions appears, and it is called Aneotrope [7].

In a wide range of applications are used the fluorinated alcohols compounds and mixtures, they can go in biochemical applications, because of the way they can support the helix conformation of proteins, they can be used to stabilize radical cations, and, perhaps the most substantial application, as solvents, for various catalytic processes and non-catalytic oxidations and cyclizations [8]. They also can be used as adjuvant components in fluoropolymer manufacture and processing, formulations of herbicides, greases, lubricants, paints, polishes, and adhesives [5]. The high solubility of respiratory gases in these compounds bring more possibilities of applications as drug delivery in liquid ventilation context, blood substitutes, and, a significant use, as a CO_2 capture [9].

With soft-SAFT this work will continue the application of J. Justino study [10][11], in his work, Justino *et al.* modeled the fluorinated alcohol family for thermodynamic and interfacial properties calculations and studied the equilibrium and surface tensions of these three mixtures: Trifluoroethanol (TFE) with Ethanol, TFE with Propanol and TFE with Butanol. The following approach to this system is to model the fluorinated alcohol family for viscosity calculations and study the behavior of mixtures with heavier fluorinated alcohol and hydrogenated alcohol. So, the mixtures studied in this work are the Heptafluorobutanol (HFB) with Butanol, Undecafluorohexanol (UFH) with Hexanol and Pentadecafluorooctanol (PDFO) with Decanol.

The number of works that studied viscosity properties of the pure fluorinated compound in the literature is very limited. For the TFE, the experimental data is vaster that for the other members of the family because it is cheaper and has a more range of applications. So, experimental viscosity data for TFE can be found in many works [12][13], and for the other members of the family, the data reported was established by Costa [14]. For other properties, the data is a little vaster for the fluorinated family, like equilibrium properties, liquid and gas densities, enthalpies, derivative properties and surface tensions [15][16][17][18].

The experimental work found for the mixtures studied in this work is very limited, having only experimental densities, excess volumes [6], surface tensions, and viscosities [14]. Almost all the experimental data comes from the team where this thesis work was developed. There are also simulations for HFB with Butanol and UFH with Hexanol with densities, viscosities, excess volumes, and enthalpies [6][19].

2. Soft-SAFT EoS

In the late 1980s, the Statistical Associating Fluid Theory was developed by Chapman, Gubbins, Jackson, and Radosz [20][21], which catch the attention of the industrial and academic society. SAFT is an EoS based on the first-order theory of Wertheim, and their approach was to describe a fluid, not only with a simple hard-sphere model, but that includes the molecular shape and association. The primary expression of SAFT EoS comes from the residual Helmholtz free energy (A^{res}) that for a system with association chains can be expressed by the sum of a reference term (A^{ref}), with both the repulsive and attractive energies, a chain term (A^{chain}) and an association contribution term (A^{assoc}):

$$\frac{A^{res}}{N_m k_B T} = \frac{A}{N_m k_B T} - \frac{A^{ideal}}{N_m k_B T} = \frac{A^{ref}}{N_m k_B T} + \frac{A^{chain}}{N_m k_B T} + \frac{A^{assoc}}{N_m k_B T} \quad (1)$$

where N_m is the number of chain molecules in the system, k_B is the Boltzmann constant and T the temperature.

In SAFT, the residual term is calculated by spheres interacting between themselves with a given potential as the reference fluid. The chain term provides information for some spheres to bond with covalent forces. Moreover, then the association term is added when it is necessary to account for association interactions between the molecules [2].

2.1. Ideal term

The ideal term (A^{ideal}) is given by the free energy of an ideal gas mixture:

$$\frac{A^{ideal}}{N_m k_B T} = \sum_{i=1}^{n_T} x_i \ln\left(\rho_m^{(i)} \Lambda_i^3\right) - 1 \quad (2)$$

where n_T are all the components of the mixture, $x_i = \frac{N_m^{(i)}}{N_m}$ the molar fraction of the components, $\rho_m^{(i)} = \frac{N_m^{(i)}}{V}$ the molecular density, Λ_i the thermal de Broglie wavelength, $N_m^{(i)}$ the number of molecules of the component, and V the volume of the system [2].

2.2. Reference term

The reference term adds to the equation the possibility of interaction between the spheres. It is in the reference term that the versions of SAFT had their most significative differences. This disparity view came from the sphere energy potential of interactions chosen as the reference term. There are three kinds of energy potential, the Hard Spheres (HS), the Square Well (SW) and the Lennard-Jones (LJ). The HS is the potential with the most straightforward approach; in this case, are only considered repulsive forces. For this reason, the spheres act like independent and cannot overlap the same space, SAFT-HS [22], and the original SAFT uses this potential as reference. In this case, an additional perturbation term is added into the equation to take into account the attractive forces between the spheres. SAFT-VR [23] uses the SW potential, and in this case, attractive and repulsive forces are considered by having a certain distance where the spheres can feel each other with a given energy until they reach the hard-sphere diameter distance and they repel each other. The soft-SAFT [1], where this work fits in, is the version that uses the LJ EoS of Johnson *et al.* [24] as reference term, where both repulsive and attractive forces are taking into account. So, the potential that accounts for the free energy of a fluid of an LJ sphere is given by:

$$\phi(r) = 4\varepsilon^{LJ}\left[\left(\frac{\sigma^{LJ}}{r}\right)^{6} - \left(\frac{\sigma^{LJ}}{r}\right)^{12}\right] \tag{3}$$

where $\phi(r)$ is the potential energy over the distance between two spheres (r), ε^{LJ} is the LJ well depth, σ^{LJ} the LJ atomic diameter and 6 and 12 are attractive and repulsive potentials, respectively [2]. In Figure 1, it is possible to identify the repulsive and attractive parts of the equation.

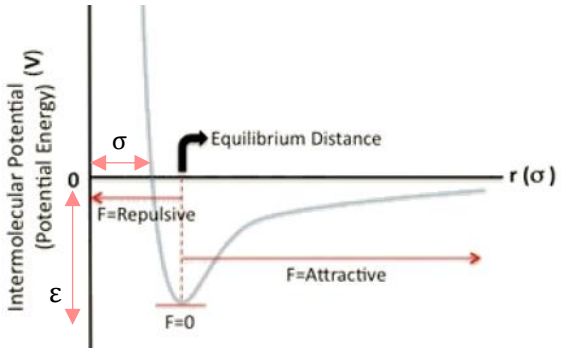

Figure 1. Lennard-Jones potential energy between two spheres.

A generalization of the soft-SAFT equation is the SAFT-γ-Mie equation [25] in which the 6-12 potential of the LJ present in soft-SAFT is generalized, and values are fitted to experimental systems.

2.3. Chain term

The chain term for homonuclear chains is given by the first-order perturbation theory and by associating spherical molecules with a specific bond length equal to σ_{ii}, the diameter of the LJ in the species i can be written as [2]:

$$\frac{A^{chain}}{N_m k_B T} = \sum_{i=1}^{n_T} x_i (1 - m_i) \ln y_R^{(ii)}(\sigma_{ii}) \tag{4}$$

where m_i is the chain length and $y_R^{(ii)}(\sigma_{ii})$ is the contact value of the cavity correlation function for spherical segments of species i in the LJ reference fluid and it is given by:

$$y_R^{(ii)}(\sigma_{ii}) = g_R^{(ii)}(\sigma_{ii}) \exp\left[\frac{\phi_{LJ}(\sigma_{ii})}{k_B T}\right] \tag{5}$$

with the $g_R^{(ii)}(\sigma_{ii})$ being the prior radial distribution function of the LJ fluid and $\phi_{LJ}(\sigma_{ii})$ the LJ potential energy [2].

2.4. Association term

The last term of the SAFT equation is the association. The intermolecular potential it is dominated at small separations by repulsive, and at large separations by attractive. These interactions are often called physical and are in the chain term where these interactions are considering. Although, for some systems, it is necessary to account for other class of interactions, called quasichemical. These attractive interactions are sturdy and highly directional, in which participating species combine to form new chemical entities. One of these interactions is hydrogen bonding.

An intermolecular hydrogen bond forms between a hydrogen-donor (negative) molecule and an electron-rich (positive) acceptor site. The hydrogen is attached to an atom (A) that is more electronegative than the hydrogen. The hydrogen acceptor (B) is also more electronegative than hydrogen, and the acceptor can also be a double or a triple bond, or it may be an aromatic hydrocarbon ring. The representation of a hydrogen bond is often as A-H · · ·B, where the dots represent the hydrogen bond [26]. It is possible to see in Figure 2 the phenomena.

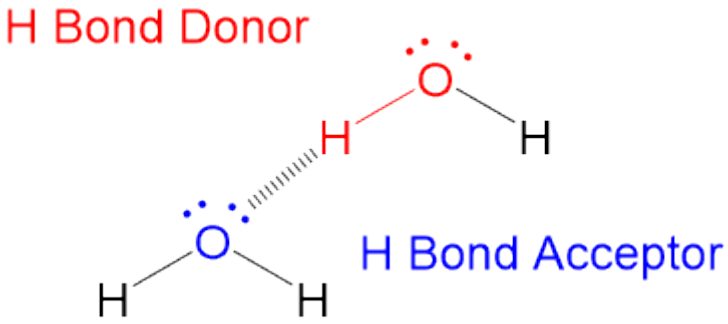

Figure 2. A hydrogen bond between two molecules of water [27].

Association is often reflected dramatically in the properties of the pure species, as boiling points, the heat of vaporization, viscosities, and surface tensions compared to similar systems with no association.

So, the association term in SAFT equations is given by the first order Wertheim's perturbation theory for associating fluid:

$$\frac{A^{assoc}}{N_m k_B T} = \sum_{i=1}^{n_T} x_i \left[\sum_{A \epsilon \Gamma^{(i)}} \left(\ln X_A^{(i)} - \frac{X_A^{(i)}}{2} \right) + \frac{n(\Gamma^{(i)})}{2} \right] \tag{6}$$

where $n(\Gamma^{(i)})$ are all the sites of each species i and $X_A^{(i)}$ is the fraction of nonbonded sites A of molecules i and can it be written as:

$$X_A^{(i)} = \frac{1}{1 + \sum_j x_j \rho_j \sum_{B \epsilon \Gamma^{(i)}} X_B^{(j)} \Delta_{AB}^{(ij)}} \tag{7}$$

where $\Delta_{AB}^{(ij)}$ is the association bond stretch between two sites:

$$\Delta_{AB}^{(ij)} = \left(\exp \left[\frac{\varepsilon_{A_{ij}B_{ij}}^{HB}}{k_B T} \right] - 1 \right) \kappa_{A_{ij}B_{ij}}^{HB} g_{LJ}^{(ij)} \tag{8}$$

where $\varepsilon_{A_{ij}B_{ij}}^{HB}$ is the energy of association between sites of two molecules, $\kappa_{A_{ij}B_{ij}}^{HB}$ is the association volume between two sites of two molecules and $g_{LJ}^{(ij)}$ it is the pair distribution function of the reference fluid [2].

2.5. Mixtures

To extend the calculations to mixtures is necessary to apply the van der Waals one-fluid theory (vdW-1f). So, the combination of vdW-1f with LJ EoS describes the Helmholtz free energy of a mixture of spherical LJ. For this theory, the residual Helmholtz free energy of a mixture is defined by the residual Helmholtz free energy of a pure speculative fluid, with parameters given by [2]:

$$\sigma^3 = \frac{\sum_i^n \sum_i^n x_i x_j m_i m_j \sigma_{ij}{}^3}{(\sum_i^n x_i m_i)^2} \tag{9}$$

$$\varepsilon\sigma^3 = \frac{\sum_i^n \sum_i^n x_i x_j m_i m_j \varepsilon_{ij} \sigma_{ij}{}^3}{(\sum_i^n x_i m_i)^2} \tag{10}$$

Moreover, the chain length follows the mixing rule:

$$m = \sum_{i=1}^{n_T} x_i m_i \tag{11}$$

Using the same rules to obtain the pair correlation function of a mixture of LJ spheres:

$$g_R^{(ii)}(r) = g_m(r^*, \rho_m{}^*, T_m{}^*) \tag{12}$$

where $g_m(r^*, \rho_m{}^*, T_m{}^*)$ is the radial distribution function for a pure LJ fluid, $r^* = \frac{r}{\sigma}$, $\rho_m{}^* = \rho_m \sigma^3$ and $T_m{}^* = \frac{k_B T}{\varepsilon}$.

For the crossed interaction parameters σ_{ij} and ε_{ij}, the crossed size and energy, respectively, are given by the Lorentz-Berthelot mixing rules:

$$\sigma_{ij} = \eta_{ij} \frac{\sigma_{ii} + \sigma_{jj}}{2} \tag{13}$$

$$\varepsilon_{ij} = \xi_{ij} \sqrt{\varepsilon_{ii} \varepsilon_{jj}} \tag{14}$$

where η_{ij} and ξ_{ij} are the binary parameters that modify the average size and energy parameters, respectively, between species i and j. When set to 1, the binary parameters do not have any contribution to the mixing rules, and calculations for mixtures are purely predictive.

At last, like the crossed interaction parameters, the association and volume parameters are given by the following mixture rules:

$$\varepsilon_{ij}^{HB} = \alpha_{ij}^{HB}\sqrt{\varepsilon_{ii}^{HB}\varepsilon_{jj}^{HB}} \tag{15}$$

$$\kappa_{ij}^{HB} = \left(\frac{\kappa_{ii}^{HB^{(1/3)}} + \kappa_{jj}^{HB^{(1/3)}}}{2}\right)^3 \tag{16}$$

where α_{ij}^{HB} is a binary parameter to adjust the cross-association energy if needed.

2.6. Properties

One of the main features of soft-SAFT is the direct calculation of the first-order properties given by the Helmholtz energy that is the pressure (P) and the chemical potential (μ_i):

$$P = \rho^2\left(\frac{\partial A}{\partial \rho}\right) \tag{17}$$

$$\mu_i = \left(\frac{\partial A}{\partial n_i}\right) \tag{18}$$

where ρ is the density and n_i the mole fraction of component i [10].

With this, soft-SAFT can predict the VLE curves of both pure and mixtures and their densities and enthalpies.

2.6.1. Vapor-Liquid Equilibrium (VLE)

Equilibrium is a static condition in which no changes occur in the macroscopic properties of a system with time. Furthermore, in engineering practice, the assumption of equilibrium is justified when it leads to results of satisfactory accuracy. An isolated system of liquid and vapor phases reaches a final state where no changes occur within the system. So, the pressure, temperature, and phase compositions reach the last values remaining fixed. However, this only happens at macroscopic levels, at microscopic level conditions are not static because molecules in a phase at a given instant are not the same molecules that later occupy the same phase [28].

The representation of the VLE of a mixture can be shown in two ways, the isothermal (constant temperature) and isobaric (constant pressure):

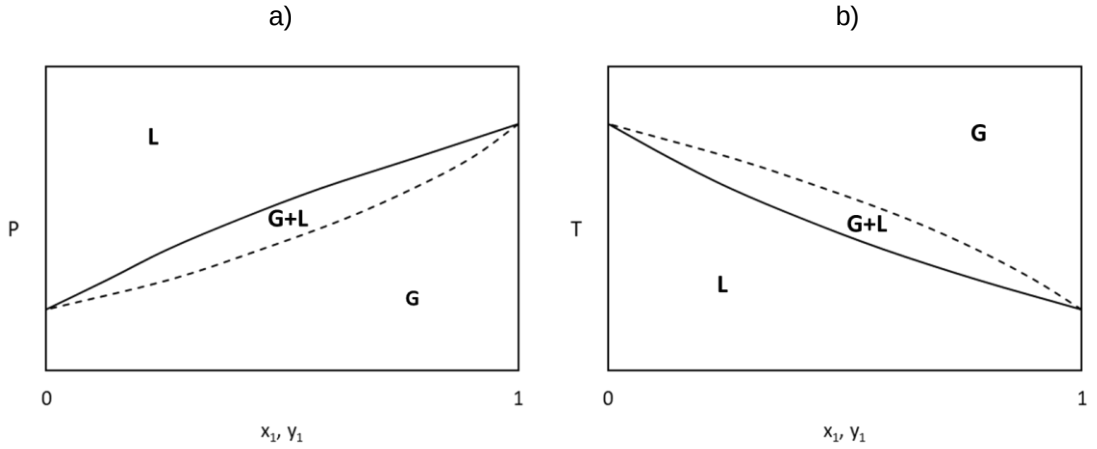

Figure 3. a) Pxy diagram example for ideal mixtures (isothermal). b) Txy diagram example for ideal mixtures (isobaric). Solid lines represent the saturated liquid (bubble line), and dotted lines represent the saturated vapor (dew line). G represents the gaseous phase, L the liquid phase, and G+L both gaseous and liquid phases at the same time.

In Figure 3, *x, y* represent the mole fraction of each component in the mixture, while the boundaries represent the pure components (x_1=0, pure component 2; x_1=1, pure component 1) being in a) the vapor pressure and in b) the boiling point. For ideal binary mixtures the bubble point is calculated applying the Raoult's law:

$$P = P_2^{sat} + (P_1^{sat} - P_2^{sat})x_1 \tag{19}$$

$$x_1 = \frac{P - P_2^{sat}}{P_1^{sat} - P_2^{sat}} \tag{20}$$

where P is the total pressure, $P_{1/2}^{sat}$ is the vapor pressure of component 1 or 2 and x_1 is the liquid composition of element 1.

The dew point calculations come from Raoult-Dalton's law:

$$P = \frac{P_1}{y_1} = \frac{P_2}{y_2} \tag{21}$$

$$y_1 = \frac{P_1}{P} = \frac{x_1 P_1^{sat}}{P_2^{sat} + (P_1^{sat} - P_2^{sat})x_1} \tag{22}$$

where $P_{1/2}$is the partial pressure of component 1or 2 and $y_{1/2}$ is the gaseous composition of elements 1 or 2.

For non-ideal mixtures, some deviations from Raoult's law come from adding two factors, the fugacity coefficient (ϕ_p) and the activity coefficient (Υ):

$$y_1 \phi_{p,1} P = x_1 \Upsilon_1 P_1^{sat} \tag{23}$$

These deviations can be positive or negative. When the cohesive forces between like components are greater than the adhesive forces between different components, the elements escape more easily from the solution, so the vapor pressure is higher than expected from the Raoult's law, having positive deviations. If the cohesive forces between like components are smaller than the adhesive forces between different components, both elements are retained in the liquid phase by attractive forces that are stronger than in the pure liquid, so the partial vapor pressure is lower [28].

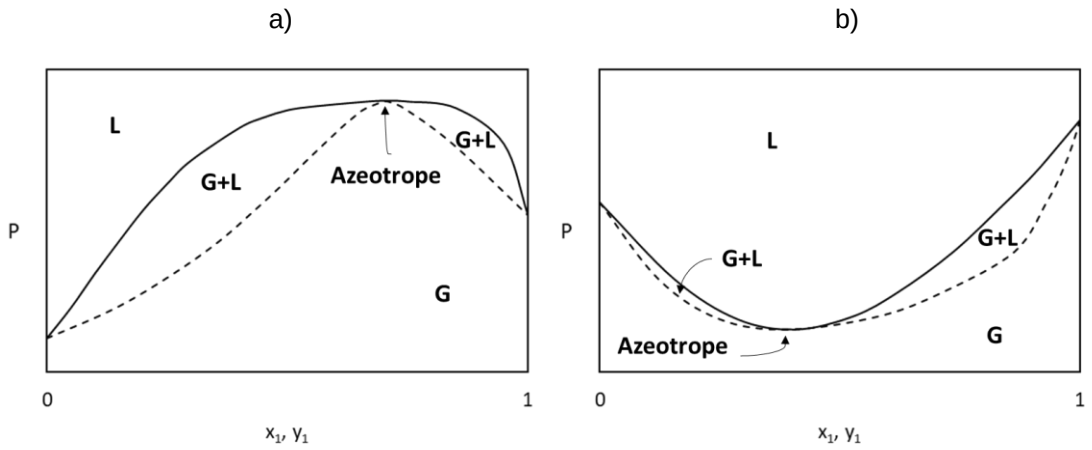

Figure 4. a) Pxy diagram of a non-ideal mixture with positive deviation. b) Pxy diagram of a non-ideal mixture with negative deviation. Solid lines represent the saturated liquid (bubble line), and dotted lines represent the saturated vapor (dew line). G represents the gaseous phase, L the liquid phase, and G+L both gaseous and liquid phases at the same time.

On the Pxy diagrams of Figure 4 is possible to see that the bubble line and the dew line intersect at one point. This point is called azeotrope, and at this composition (x1=y1), pressure and temperature, the composition in the vapor and the liquid are identical, the mixture has the same behavior as a pure component.

2.6.2. Density

Density is an essential characteristic of substances, not only because of her physical importance but also because density is crucial for the prediction of other fluid properties, like viscosity and surface tension. Density can also reveal the phase of a substance. Densities of gases are much less than of liquids because, in gases, the atoms have large amounts of empty space between them compering to the liquid.

By definition is mass per unit of volume:

$$\rho = \frac{m}{V} \tag{24}$$

where ρ represents the density, m the mass, and V the volume.

The components studied in this work are homogeneous; this means that the density at all points of the substance is equal, unlike heterogeneous elements where its density varies between different regions.

For mixtures density is the sum of mass concentrations of all the components:

$$\rho = \sum_i \frac{m_i}{V} \tag{25}$$

Furthermore, expressed as a function of the densities of the pure components in the mixture and their volume participation, it is possible to determinate the excess molar volumes:

$$\rho = \sum_i \rho_i \frac{V_i}{V} = \sum_i \rho_i \frac{V_i}{\sum_i V_i + \sum_i V_i^E} \tag{26}$$

where V^E represents the excess volume that quantifies the non-ideal behavior of a real mixture, being the difference between the value in a real mixture and the value that would exist in an ideal solution under the same conditions.

2.6.3. Enthalpy

Enthalpy comprises a system's internal energy, which is the energy necessary to create the system, plus the amount of work essential to make room for it by displacing its environment and establishing its volume and pressure.

Subsequently, the enthalpy (H) is defined as [26]:

$$\mathrm{H} = \mathrm{U} + \mathrm{PV} \tag{27}$$

where U is the internal energy, P the pressure, and V the volume.

Enthalpy like U, P, and V is a state function, and similar to other state functions, the change in enthalpy $(\Delta\mathrm{H})$ is independent of the path between any pair of initial and final states.

At constant pressure, the change in enthalpy is equal to the heat released or absorbed by the system (q). So, for $\Delta\mathrm{H} < 0$, the system is exothermic, for $\Delta\mathrm{H} > 0$, is endothermic, and for $\Delta\mathrm{H} = 0$, is thermoneutral.

$$\mathbf{\Delta H = q} \tag{28}$$

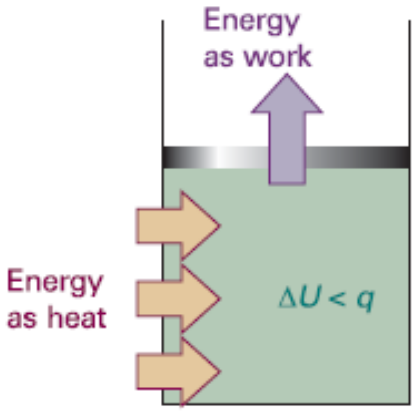

Figure 5. Illustration of the change in internal energy [26].

Figure 5 shows that when a system is subjected to constant pressure and is free to change its volume, some of the energy supplied as heat may escape back into the surroundings as work. In such a case, the change in internal energy is smaller than the energy supplied as heat [26].

The excess enthalpy quantifies the non-ideal behavior of a real mixture, being the difference between the value in a real mixture and the value that would exist in an ideal solution under the same conditions.

2.6.4. Second derivative properties

soft-SAFT can also provide second derivatives of the Helmholtz pressure and energy, just by applying their definition to the original equation, as follows [29]:

$$C_v = -T\left(\frac{\partial^2 A}{\partial T^2}\right)_v \tag{29}$$

$$k_T^{-1} = \rho\left(\frac{\partial P}{\partial \rho}\right)_T \tag{30}$$

$$\mu_{JT} = T\left(\frac{\partial P}{\partial T}\right)_v - \rho\left(\frac{\partial P}{\partial \rho}\right)_T \tag{31}$$

$$\alpha_E = k_T\left(\frac{\partial P}{\partial T}\right)_\rho \tag{32}$$

$$C_p = C_v + \frac{T\alpha^2}{k_T \rho} \tag{33}$$

$$c = \sqrt{\frac{C_p}{C_v}\left(\frac{\partial P}{\partial \rho}\right)_T} \tag{34}$$

where C_v is the isochoric heat capacity, k_T is the reduced bulk modulus, μ_{JT} is the Joule-Thomson coefficient, α_E is the thermal expansion coefficient, C_p is the isobaric heat capacity, and c is the speed of sound.

3. Density Gradient Theory (DGT)

By joining the Density Gradient Theory (DGT) with soft-SAFT is possible to calculate the interfacial properties of a compound or a mixture [30][31][32].

An interface is a physical boundary between two different phases, and a liquid-vapor interface is commonly called surface. The surface has interesting properties since the behavior of the components on the surface is entirely different, as in the bulk. Some of these properties are surface tension, adsorption, and density profiles. Figure 6 represents a simple illustration of a simulation of the interface.

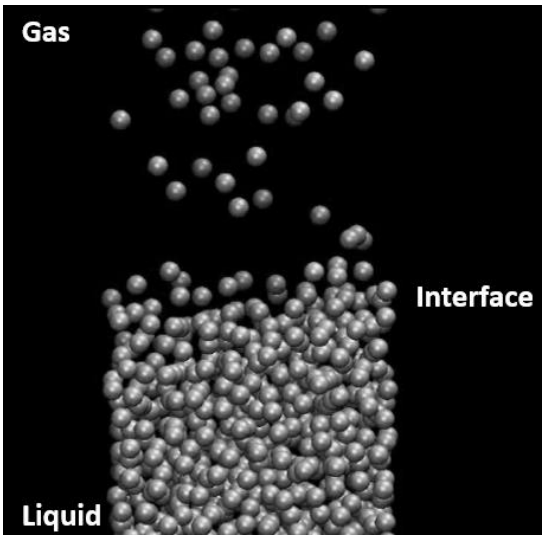

Figure 6. Illustration of a simulation of xenon at the interface.

The cohesive forces between liquid molecules are responsible for the phenomenon known as surface tension. At the surface, the molecules do not have other like molecules on all sides of them, and because of this, they cohere more strongly to those directly associated with them on the surface. A surface film is formed, making it more challenging to move through the surface than in the bulk. So, the surface tension is the force per unit of length necessary to break this film [33]. The work done is equal to:

$$\mathrm{Work} = \gamma \, \mathrm{l} \, \mathrm{dx} = \gamma \, \mathrm{dA} \tag{35}$$

where γ represents the surface tension, l the length and dx is the distance being $\mathrm{l} \, \mathrm{dx} = \mathrm{dA}$ the changing in the area.

The Gibbs equation can describe the surface tension having:

$$dG = VdP - SdT + \gamma\, dA + \sum_i \mu_i\, n_i = dW \tag{36}$$

where G is the Gibbs free energy, V the volume, P the pressure, S the entropy, T the temperature, i the component, A the surface area, μ the chemical potential, n the number of moles, W the work.

At constant pressure, temperature and number of moles the surface tension is given by:

$$\gamma = \left(\frac{dW}{dA}\right)_{P,T,n} \tag{37}$$

For mixtures, the description of the surface tension is more complicated since there are components that prefer to stay in the bulk and others that prefer to migrate to the interface. For example, the surfactants prefer to migrate to the interface, and when oriented the hydrophobic site out of the interface and the hydrophilic site toward the interface, and by doing this the surface tension decreases.

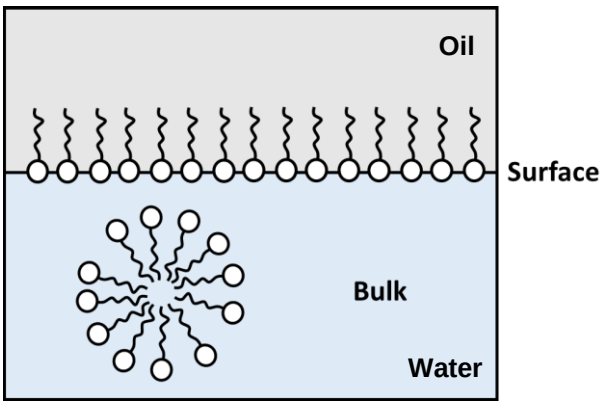

Figure 7. Representation of the surfactant molecules with a polar head and a hydrophobic tail in the bulk and at the interface between water and oil.

If the concentration of one compound (i) is uniform right up to the interface, from its volume is possible to conclude that exist a certain amount of compound i in the liquid phase ($n_i\,(L)$) and in the gaseous phase ($n_i\,(G)$). Although, species can accumulate at the interface ($n_i\,(I)$). So, if the total amount of component i is n_i the amount at the interface is equal to [26]:

$$n_i\,(I) = n_i\, - [n_i\,(L) + n_i\,(G)] \tag{38}$$

The surface excess (Γ_i) express this difference, also known by adsorption. Furthermore, by Equation (36), at constant temperature and pressure, and seeking a connection between the change of surface tension and the change of composition at the interface we have:

$$A\,d\gamma + \sum_i n_i\,(I)\,d\mu_i = 0 \tag{39}$$

$$\sum_i \Gamma_i\,d\mu_i = d\gamma \tag{40}$$

$$\Gamma_i = \frac{n_i\,(I)}{A} \tag{41}$$

For binary mixtures, since Γ_1 and Γ_2 are defined relative to an arbitrarily chosen dividing surface, it is possible to place the surface so that Γ_1 or Γ_2 is equal to 0, as illustrated in Figure 8.

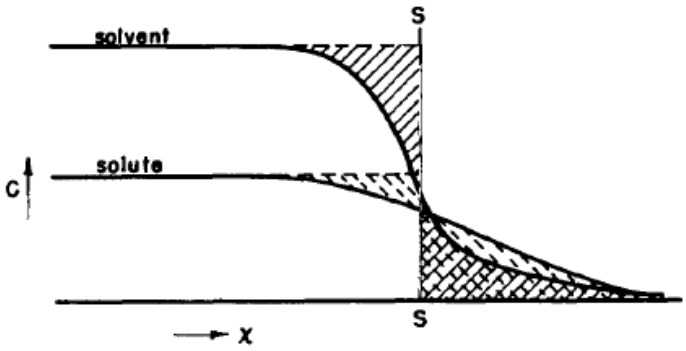

Figure 8. Schematic illustration of surface excess [33].

In Figure 8, the surface line it has drawn so that the areas with stokes are equal, so the surface excess of the solvent is zero. The area with dashed strokes, which lies to the right of the dividing surface minus the smaller similarly shaded area to the left corresponds to the (in this case positive) surface excess of solute. So, in this case, if the solvent is component 1 and the solute the 2 [33]:

$$d\gamma = -\Gamma_1\,d\mu_1 - \Gamma_2\,d\mu_2 \tag{42}$$

$$\text{If } \Gamma_1 = 0, \qquad \Gamma_2^1 = -\left(\frac{d\gamma}{d\mu_2}\right)_{T,P} \tag{43}$$

The interface is also a small region with a certain thickness (Δz), where properties, like density, vary continuously from liquid to gas. So, the representation of the density over z is called density profile.

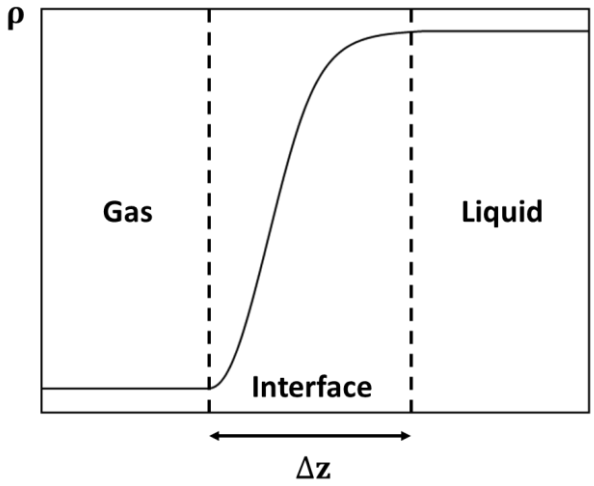

Figure 9. Molecular density profile representation with no adsorption at the interface.

Generally, in a mixture, are components that prefer to stay in the bulk (negative adsorption) and components that prefer to migrate to the interface (positive adsorption), In the negative adsorption, the density at the interface is lower than in the bulk and, consequently, in the positive adsorption, the density at the interface is higher than in the bulk.

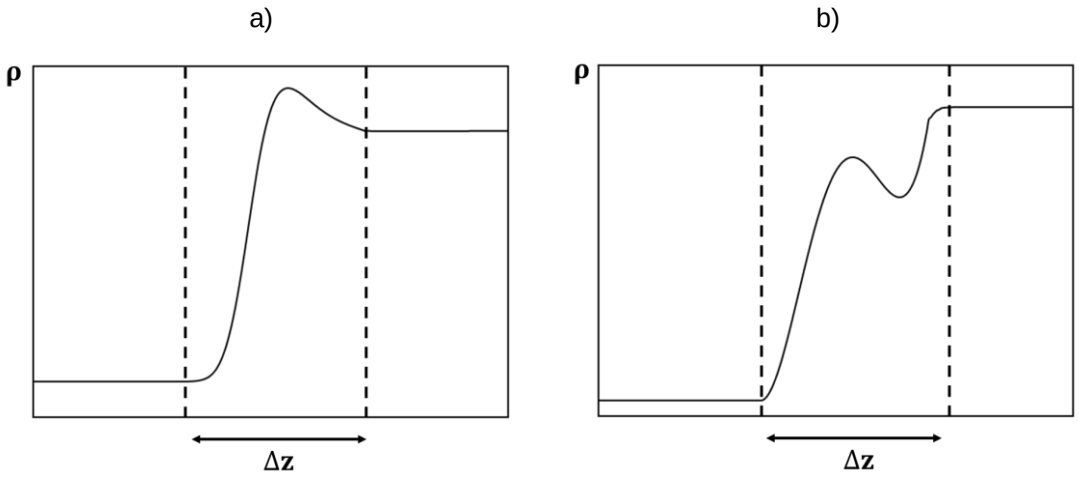

Figure 10. Schematic density profile diagrams. a) Positive adsorption. b) Negative adsorption.

So, Cahn and Hilliard re-discovered the density gradient theory (DGT) [34] of the van der Waals and expanded the Helmholtz free energy density ($\tilde{a}$) in a Taylor series about $\tilde{a}_0(\tilde{\rho})$, the Helmholtz free energy of the homogeneous fluid at the local density $\tilde{\rho}$, and shorten after the second-order term.

$$\tilde{A} = \int \left[\tilde{a}_0(\tilde{\rho}) + \sum_i \sum_j \frac{1}{2} \tilde{c}_{ij} \nabla\tilde{\rho}_i \nabla\tilde{\rho}_j \right] d^3\tilde{r} \tag{44}$$

where $\nabla\tilde{\rho}_i$ and $\nabla\tilde{\rho}_j$ are the molar density gradient of compounds i and j and $\tilde{c}_{ij}$ is the coefficient of proportionality called the influence parameter.

The influence parameter was akin to the mean square range of the direct correlation function $C_{ij,0}$ of a homogeneous fluid:

$$\tilde{c}_{ij} = \frac{\tilde{T}}{6} \int \tilde{r}^2 C_{ij,0}(\tilde{r}, \tilde{\rho}) d^3\tilde{r} \tag{45}$$

However, for the appliance, the coefficient is fitted using experimental data of surface tensions of pure components. Moreover, for mixtures, the parameter is given by the geometric mean combination rule:

$$\tilde{c}_{ij} = \beta_{ij} \sqrt{\tilde{c}_{ii} \tilde{c}_{jj}} \tag{46}$$

where β_{ij} is another binary parameter to adjust possible deviations.

Then, by minimization of the total free energy of the system is possible to obtain the density profiles. Knowing that the chemical potential of a species remains constant across the interface and applying this in Equation (44):

$$\sum_j \nabla \cdot \left(\tilde{c}_{ij} \nabla\tilde{\rho}_j \right) - \frac{1}{2} \sum_k \sum_j \frac{\partial \tilde{c}_{kj}}{\partial \tilde{\rho}_j} \nabla\tilde{\rho}_k \cdot \nabla\tilde{\rho}_j = \frac{\partial(\tilde{a}_0(\tilde{\rho}) - \sum_i \tilde{\rho}_j \tilde{\mu}_{0j}}{\nabla\tilde{\rho}_i} \tag{47}$$

The surface tension is a consequence of the density profile, and by assuming a planar interface and ignoring the influence parameter dependence, the surface tension can relate with the density gradient in an equation derived from Equation (47):

$$\tilde{\gamma} = \sum_{i}\sum_{j}\int \tilde{c}_{ij}\frac{\partial\tilde{\rho}_i}{\partial\tilde{z}}\frac{\partial\tilde{\rho}_j}{\partial\tilde{z}}\partial\tilde{z} = 2\int_{-\infty}^{+\infty}\left[\tilde{a}_0(\tilde{\rho}) - \sum_{i}\tilde{\rho}_i\tilde{\mu}_{0i} - \tilde{p}_0\right]\partial\tilde{z} \tag{48}$$

where μ_{0i} is the equilibrium chemical potential, p_0 the equilibrium pressure and z the direction perpendicular to the interface.

Then, expressing Equation (48) in terms of density space, by transforming from location space, Poser and Sanchez provide was a way to calculate the density profiles:

$$\tilde{z} = \tilde{z}_0 + \int_{\tilde{\rho}_j(\tilde{z}_0)}^{\tilde{\rho}_j(\tilde{z})}\sqrt{\frac{\tilde{c}'}{\Delta\widetilde{\Omega}(\tilde{\rho}_i,\tilde{\rho}_j)}}\partial\tilde{\rho}_j \tag{49}$$

where $\tilde{z}_0$ is the origin,$\Delta\widetilde{\Omega}(\tilde{\rho}_i,\tilde{\rho}_j)$ is the reduced grans thermodynamic potential and $\tilde{c}'$ is a consequence of the influence parameter of each pure component and the density profile and is given by [35]:

$$\tilde{c}' = \tilde{c}_{jj+} + 2\tilde{c}_{ij}\left(\frac{\partial\tilde{\rho}_i}{\partial\tilde{\rho}_j}\right) + \tilde{c}_{ii}\left(\frac{\partial\tilde{\rho}_i}{\partial\tilde{\rho}_j}\right)^2 \tag{50}$$

Besides the calculations of the surface tension, the density profiles allow calculating the adsorption of molecules in the interface. So, the adsorption of compound i on j is calculated using the equation defined by Gibbs.

$$\Gamma_{ij} = -\alpha_i\int_{-\infty}^{+\infty}\Delta C(z)dz \tag{51}$$

where $\Delta C(z)$ is the symmetrical interface segregation at symmetrical concentrations α_i:

$$\Delta C(z) = \frac{\rho_j(z) - \rho_j^L}{\alpha_j} - \frac{\rho_i(z) - \rho_i^L}{\alpha_i} \tag{52}$$

$$\alpha_{i/j} = \frac{\rho_{i/j}^L - \rho_{i/j}^v}{\left(\rho_i^L + \rho_j^L\right) - \left(\rho_i^v + \rho_j^v\right)} \tag{53}$$

where $\rho_{i/j}(z)$ is the density of each component over z and $\rho_{i/j}^L$ and $\rho_{i/j}^v$ are the densities of each component in liquid and vapor face, respectively. Because the adsorption calculated is of component i relative to component j, the adsorption of component j is assumed to be zero.

4. Free-Volume Theory (FTV)

To predict viscosities soft-SAFT can be, once more, copulated with another theoretical model, and the most popular to estimate viscosities is the free-volume theory (FTV) [36][37][38][39].

When a liquid flow, it has an internal resistance to flow, and viscosity is the measure of this resistance to flow or shear. Viscosity can be expressed in two distant forms, the absolute or dynamic viscosity and the kinematic viscosity [40].

The dynamic viscosity is the tangential force per unit area needed to slide one layer (A) against another layer (B) when the two layers are maintained at a unit distance, as shown in Figure 11.

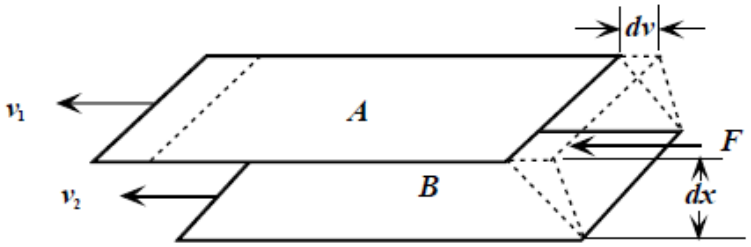

Figure 11. Shear of a liquid film [40].

Force F causes layers A and B to slide at velocities ν_1 and ν_2, respectively. If σ is the shear stress and e is the strain rate, we have:

$$\sigma = \eta \times e \tag{54}$$

The definition of the strain rate is:

$$e = \frac{1}{l}\frac{dx}{dt} = \frac{\nu}{l} \tag{55}$$

where l is the length, t is the time and $\frac{dl}{dt}$ the velocity (ν).

So, the dynamic viscosity (η) is:

$$\eta = \sigma\frac{l}{\nu} \tag{56}$$

Kinematic viscosity is the ratio of the dynamic viscosity to the density:

$$\upsilon = \frac{\eta}{\rho} \tag{57}$$

The FTV model was proposed in 2001 by Allal and co-workers [41][42] and can be used for dense and low-dense fluids by associate the viscosity with the fluid molecular structure.

In this theory, the viscosity (η) is equal to the summation of two terms:

$$\eta = \eta_0 + \Delta\eta \tag{58}$$

where η_0 is the viscosity of the dilute term, and $\Delta\eta$ is the dense correction term.

The dilute term corresponds to the viscosity of the fluid as if it was in a gaseous state or at a very low density, and is given by:

$$\eta_0 = 0.040785 \frac{\sqrt{M_W T}}{v_c^{2/3} \Omega^*(T^*)} F_c \tag{59}$$

where M_W is the molecular weight, T is the temperature, v_c is the critical volume, $\Omega^*(T^*)$ is the reduced collision integral for the LJ potential and F_c is the empirical correction factor that includes the effect of chain bonding, hydrogen bonding, and polarity.

The reduced collision integral for the LJ potential $\Omega^*(T^*)$ is given by:

$$\begin{aligned}\Omega^*(2;2) = {} & \frac{1.16145}{T^{*0.14874}} + \frac{0.52487}{\exp(0.77320\, T^*)} + \frac{2.16178}{\exp(2.43787\, T^*)} \\ & - 6.435 \times 10^{-4}\, T^{*0.14874} \sin(18.0323\, T^{*-0.76830} - 7.27371)\end{aligned} \tag{60}$$

where T^* is a dimensionless temperature $T^* = 1.2593\, T_r$, being T_r the reduced temperature connected to the critical temperature of the fluid.

The F_c, in Equation (59), is the empirical correction factor that includes the effect of chain bonding, hydrogen bonding, and polarity and is given by:

$$F_c = 1 - 0.275\, \omega - 0.059035\, \mu_r^4 - k \tag{61}$$

where ω is the acentric factor, μ_r is the reduced dipole moment, and k is an empirical parameter that accounts for the hydrogen bonding formation.

For the dense correction term, two things are taking into consideration, the linking of viscosity with the microstructure of the fluid and his dependent on the empty space between molecules. Furthermore, it is here that the free-volume fraction has his representation. With these two sides, the dense term can be given by:

$$\Delta\eta = 10^{-4}\rho N_A L^2 \zeta_0 \exp\left(\frac{B}{f_v}\right) \tag{62}$$

where ρ is the density, N_A the Avogadro's number, L^2 is an average quadratic length related to the size of the molecule, ζ_0 is the friction coefficient related to the diffusion process and the mobility of the molecule, B is a parameter related to the free-volume overlap among the molecules and f_v is the free-volume fraction.

The free-volume fraction is given by:

$$f_v = \left(\frac{RT}{E}\right)^{3/2} \tag{63}$$

where R is the universal constant for gases and E is the potential energy of interaction,

$$E = \frac{10^3 P}{\rho} + \alpha\rho M_W \tag{64}$$

being P the system pressure and α an activation energy parameter.

The friction coefficient is also related to the energy of interaction:

$$\zeta_0 = 10^{10}\frac{E}{N_A b_f}\left(\frac{10^{-3}M_W}{3RT}\right)^{1/2} \tag{65}$$

where b_f is the length of dissipation.

Then, by combining all the equations, $\Delta\eta$ is given by:

$$\Delta\eta = L_v(0.1P + 10^{-4}\alpha\rho^2 M_W)\sqrt{\frac{10^{-3}M_W}{3RT}}\exp\left[B\left(\frac{10^3 P + \alpha\rho^2 M_W}{\rho RT}\right)^{3/2}\right] \tag{66}$$

being $L_v = \frac{L^2}{b_f}$.

For the final equation, the system requires three different parameters, α that is the proportionality between the energy barrier and the density, B that is the free-volume overlap and L_v that is a length parameter related to the structure of the molecules and the characteristic relaxation.

To extend this equation for mixtures is only necessary to change the three parameters with the corresponding mixing rules. These are chosen simple linear compositional of the Lorentz type:

$$\alpha_{mixt} = \sum_{i=1}^{n} x_i \alpha_i \tag{67}$$

$$\frac{1}{B_{mixt}} = \sum_{i=1}^{n} \frac{x_i}{B_i} \tag{68}$$

$$\frac{1}{L_{v,mixt}} = \sum_{i=1}^{n} \frac{x_i}{L_{v,i}} \tag{69}$$

where x_i is the molar composition of each compound. This approach is used to avoid any binary adjustable parameter.

5. Molecular Models and Transferable Parameters

Soft-SAFT needs three parameters to describe a simple, non-associating, pure fluid: m, the chain length, σ, the diameter of the groups forming the chain and ε, the energy of interaction between them. In the case of associating molecules is necessary two more parameters: ε^{HB} and κ^{HB}. It is possible to see the illustration of these parameters in Figure 12. All these parameters were fitted using experimental data available for vapor pressure and saturated liquid density over a range of temperatures. Than for mixtures, three binary adjustable parameters: η_{ij}, ξ_{ij} and α_{ij}^{HB} can be used to take into account the non-ideality in terms of size (volume), energy, and energy of association.

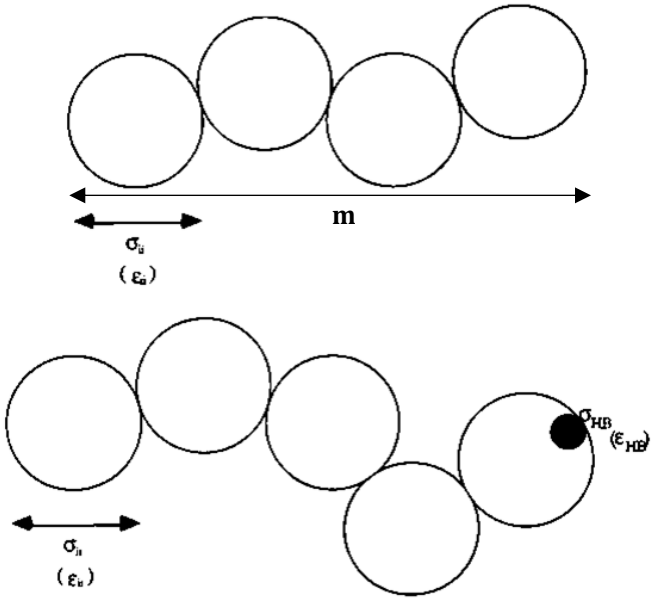

Figure 12. a) Two-dimensional view of the homonuclear associating chain. The large circles represent the Lennard-Jones cores, and the small circle is an associating site. (b) Two-dimensional view of a heteronuclear nonassociating Lennard-Jones chain with different segment sizes and dispersive energies [2].

For interfacial properties calculation and combining soft-SAFT with DGT, one more parameter is necessary, c, the influence parameter, usually fitted using experimental surface tensions. Then, to describe the interface properties of mixtures is necessary one more binary adjustable parameter, β_{ij}, in case the mixture is highly non-ideal with to interfacial tensions. At last, for viscosity calculations, soft-SAFT with FTV needs three parameters for the FVT: α, B and L_v. These parameters are fitted using experimental viscosities for pure substances. Moreover, for mixtures, none additional parameters are needed when the Spider-Web approach is used [39].

In this work, the parameters to describe the thermodynamic properties and interfacial properties of the fluorinated alcohols family were fitted in previous work by Justino [11], and have been used here in a transferable manner:

Table 1. Molecular and influence parameters for the fluorinated alcohols family used in this work

Molecule	$\mathbf{m}$	$\boldsymbol{\sigma}$ (Å)	$\boldsymbol{\varepsilon}$ (K)	$\boldsymbol{\varepsilon^{HB}}$(K)	$\boldsymbol{\kappa^{HB}}$(Å^3)	$\mathbf{c}$ (Jm^5/mol^2)
TFE	1.774	3.84	214.0	3424	2882	9.58E-20
PFP	1.979	4.13	225.1	3450	2250	1.46E-19
HFB	2.210	4.32	239.0	3450	2250	2.34E-19
NFP	2.445	4.46	250.0	3450	2250	3.41E-19
UFH	2.690	4.56	259.6	3450	2250	4.76E-19
TRFH	2.956	4.64	266.0	3450	2250	6.62E-19

Furthermore, for the hydrogenated alcohols family, the same was done where the parameters to describe the thermodynamic properties come from a previous work done by Pàmies [35], and the parameters to calculate the interface properties come from the work of Justino [11]. The fitting of these parameters are for a temperature equal to 0.55 times the critical temperature of each alcohol compound, and the parameters for viscosity calculation come from Llovell *et al.* [38].

Table 2. Molecular and influence parameters for the alcohols family used in this work

Molecule	$\mathbf{m}$	$\boldsymbol{\sigma}$ (Å)	$\boldsymbol{\varepsilon}$ (K)	$\boldsymbol{\varepsilon^{HB}}$(K)	$\boldsymbol{\kappa^{HB}}$(Å^3)	$\mathbf{c}$ (Jm^5/mol^2)
methanol	1.491	3.375	220.4	3213	4847	2.29E-20
ethanol	1.74	3.635	234.8	3387	2641	5.21E-20
1-propanol	1.971	3.808	252.7	3450	2250	9.69E-20
1-butanol	2.21	3.94	269.2	3450	2250	1.54E-19
1-pentanol	2.42	4.051	283.7	3450	2250	2.29E-19
1-hexanol	2.676	4.119	291.6	3450	2250	3.28E-19
1-heptanol	2.9	4.18	299.4	3450	2250	4.45E-19
1-octanol	3.148	4.218	305.8	3450	2250	5.78E-19

Table 3. Viscosity parameters for the alcohols family used in this work

Molecule	$\boldsymbol{\alpha}$ (Jm^3/mol kg)	$\mathbf{B}$	$\mathbf{L_v}$(Å)
methanol	165.6	0.004362	0.1537
ethanol	230	0.003831	0.1286
1-propanol	285	0.003551	0.09928
1-butanol	342.1	0.002948	0.08876
1-hexanol	460	0.00225	0.06472
1-octanol	564	0.00188	0.04482

It is possible to see that the three molecular parameters m, σ, and ε increase linearly with the molecular weight or the carbon number, and for that reason is possible to have linear correlations to describe the tendency of the parameters. The c parameter can be described by a 2nd-grade correlation. And, the viscosity parameters α, B and L_v can be described most of the time or by a linear or an exponential correlation. In Appendix A are exposed all the correlations used for these to families. This allows the prediction for compounds of the same family not included in the fitting procedure.

6. Results and Discussion

6.1. Viscosity parameterization and results of the pure components

To study the viscosities of the mixtures is necessary to have all the parameters that describe the pure components. For this work, the only parameters left to fit are the viscosities parameters of the fluorinated alcohols family, for which it is necessary to have experimental viscosities data. Experimental data for this family is not vast, but data for TFE come from Salgado *et al.* [12]; data for PFP, HFB, and UFH are taken from Costa [14] and for TRFH from Afonso [19]. All this data was measured at the atmospheric pressure and for a range of temperatures between 278 and 353 K.

In order to fit the parameters, we have used the Spider-Web Methodology introduced by Cané, Llovell, and Vega [39]. In this method, the experimental viscosity for the pure and mixtures is used to obtain the parameters that describe the pure components. So, the final values of the fitting are in Table 4, and the results plotted in Figure 13.

Table 4. Molecular, influence, and viscosity parameters for the fluorinated alcohols family.

Molecule	m	σ (Å)	ε (K)	ε^{HB}(K)	κ^{HB}(Å^3)	c (Jm^5/mol^2)	α ($Jm^3/mol\,kg$)	B	L_v(Å)
TFE	1.774	3.84	214.0	3424	2882	9.58E-20	317.5	0.001476	0.02573
PFP	1.979	4.13	225.1	3450	2250	1.46E-19	372.7	0.001268	0.01888
HFB	2.210	4.32	239.0	3450	2250	2.34E-19	437.7	0.00104	0.01474
UFH	2.690	4.56	259.6	3450	2250	4.76E-19	575.0	0.0007643	0.00899
TRFH	2.956	4.64	266.0	3450	2250	6.62E-19	656.4	0.0006719	0.007021

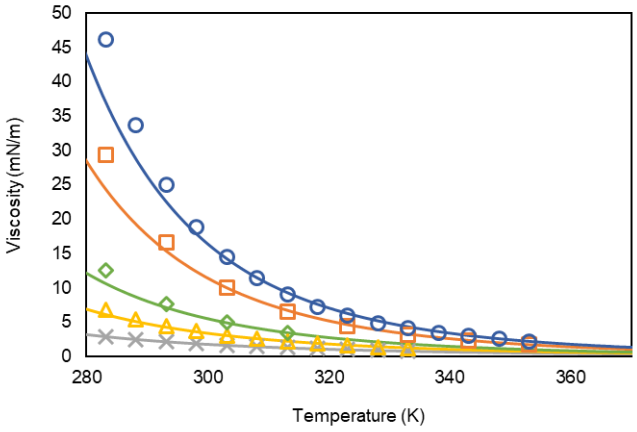

Figure 13. Viscosity for the fluorinated alcohols family over the temperature at 0.1013 MPa. Solid lines represent soft-SAFT+FTV and symbols the experimental data [12][14][19]. ○ **TFE**, □ **PFP**, ◊ **HFB**, Δ **UFH**, and X **TRFH**.

With the analysis of the viscosity parameters, it is possible to identify a trend in the values, allowing to establish correlations with the molecular weight for each parameter. For parameter α, the values tend to increase linearly with the molecular weight. Although parameters B and L_v tend to decrease with the molecular weight, but an exponential function describes better the values. And, it is possible to see that the parameters B and L_v decreases are more pronounced as observed for the alcohols, and this is, as expected because a hydrogen atom is substituted by a fluorine atom. Figure 14, Figure 15, and Figure 16 shown these three parameters and the correspondents correlations with the molecular weight.

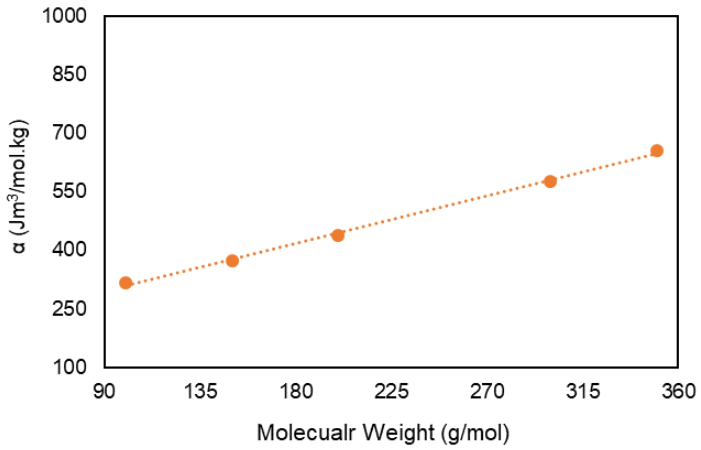

Figure 14. Viscosity parameter α correlation. Symbols represent α values and the dotted line, a linear regression.

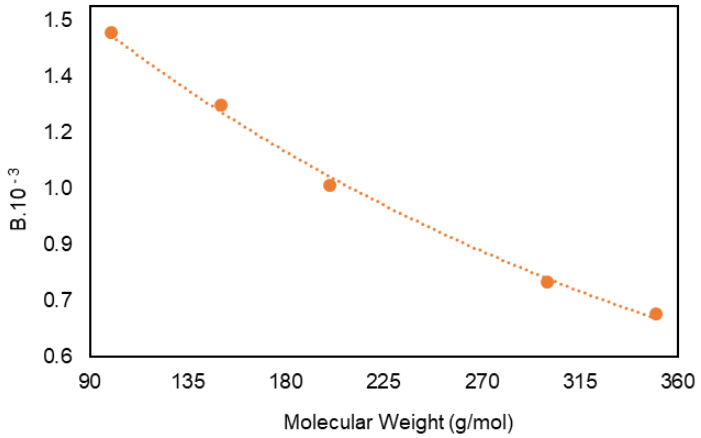

Figure 15. Viscosity parameter B correlation. Symbols represent B values and the dotted line, an exponential regression.

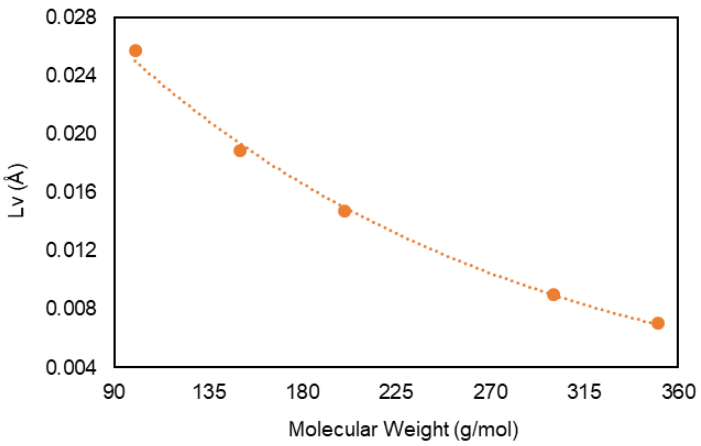

Figure 16. Viscosity parameter L_v correlation. Symbols represent L_v values and the dotted line, an exponential regression.

Being the correlation for each parameter:

$$\alpha = 1.358M_W + 173.1 \quad (70)$$

$$B = 2.019 \times 10^{-3} e^{-3.193 \times 10^{-3} M_W} \quad (71)$$

$$L_v = 4.171 \times 10^{-2} e^{-5.119 \times 10^{-3} M_W} \quad (72)$$

6.2. Mixtures

6.2.1. TFE with Hydrogenated Alcohols

As follows, Justino and Silva *et al.* work [11] and before initiate, the study of the three mixtures proposed. It was calculated the surface tensions and adsorptions of TFE with heavier hydrogenated alcohols, in order to observe what the model predict for these mixtures. In order to obtain these values, the adjustable parameters used were the same proposed in [11] fitted for his mixtures (η_{ij}=1.012, $\xi_{ij} = 1$, $\alpha_{ij}^{HB} = 1.035$ and $\beta_{ij} = 0.8$).

The calculation of the adsorptions was made applying Equation (51) through an Excel file developed in the framework of this thesis. To validate the procedure of this work, the adsorption calculations presented by Justino in reference [10] with another software and the ones implementing Equation (51) from this work were compared, and results are compared in Figure 17.

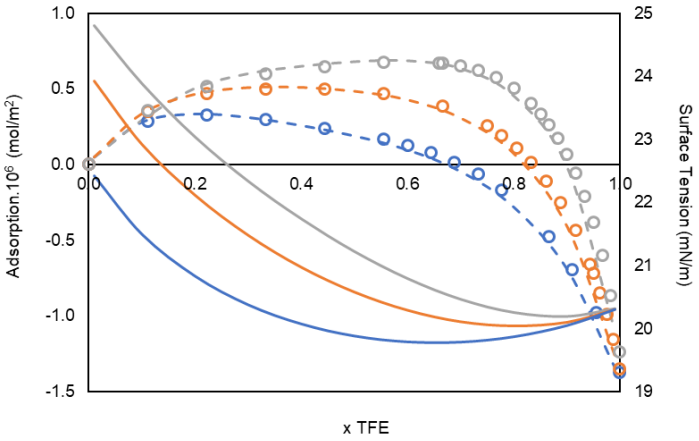

Figure 17. Surface tension (solid line), adsorption (dashed line), and adsorptions from Justino (symbols) and from this work (lines) of TFE with Ethanol, Propanol, and Butanol. **TFE + Ethanol**, **TFE + Propanol**, **TFE + Butanol**.

Once the procedure was assessed, predictions for the mixtures of TFE with Pentanol, Hexanol, and Heptanol were made in this work, and results are presented in Figure 18.

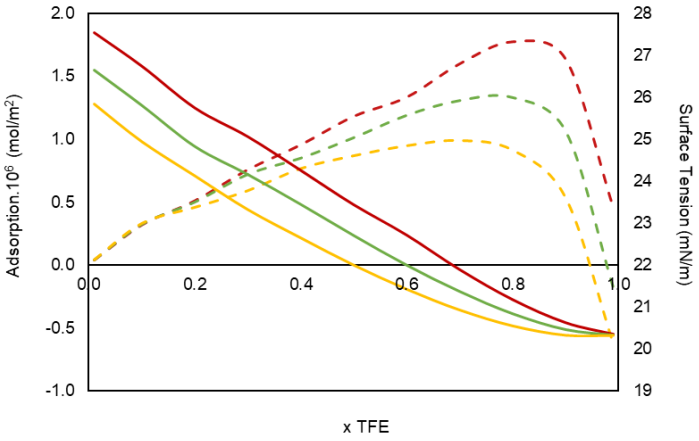

Figure 18. Surface tension (solid line) and adsorption (dashed line) of TFE with Pentanol, Hexanol, and Heptanol. **TFE + Pentanol**, **TFE + Hexanol** and **TFE + Heptanol**.

The mixtures of TFE with heavier hydrogenated alcohols show that the aneotrope concentration previously observed [11] rises with the carbon number of the hydrogenated alcohols until the aneotrope no longer exists for the TFE with Heptanol mixture. The rate of migration of TFE is higher as heavier is the hydrogenated alcohol, and the decrease of adsorption is increasingly at higher TFE concentration, which means that it is necessary to have more TFE at the surface to decrease the surface tension for mixtures with heavier hydrogenated alcohols.

6.2.2. Hexane with Perfluorohexane

To study the mixtures of HFB with Butanol, UFH with Hexanol and PDFO with Decanol first was necessary to implement the model for the Hexane with Perfluorohexane. This strategy is needed since this mixture is close to the UFH with Hexanol and for mixtures of heavier components the influence of the OH group is less and less meaningful, while in [11] the mixtures studied had a small carbon chain, and the OH group have a more substantial impact on the properties of the mixtures.

But studying first a similar mixture and fit the adjustable parameters of the crossed interactions (η_{ij} and ξ_{ij}) and them using these parameters and fitting only the adjustable parameter of association (α_{ij}^{HB}) for the fluorinated and hydrogenated alcohols mixtures, it seems more reliable and meaningful in the way the parameters are transferred.

Following a systematic approach, all the parameters needed for this mixture were taken from previous works and used in a transferable manner, with no fitting. Hence, the molecular parameters for Hexane and Perfluorohexane were taken from Pàmies work [35], the influence parameter of hexane from Vilaseca, and Vega [30] and of perfluorohexane from Dias *et al.* [43], and the viscosity parameters of hexane come from Llovell, Marcos and Vega [36]. The viscosity parameters for perfluorohexane were fitted using experimental data from reference [44].

Table 5. Molecular, influence, and viscosity parameters of hexane and perfluorohexane.

Parameter	Hexane	Perfluorohexane
$\mathbf{m}$	2.832	2.832
$\boldsymbol{\sigma}$ (Å)	3.929	4.449
$\boldsymbol{\varepsilon}$ $(\mathbf{K})$	254.4	230.2
$\mathbf{c}$ $(\mathbf{Jm^5/mol^2})$	3.556E-9	6.960E-19
$\boldsymbol{\alpha}$ $(\mathbf{Jm^3/mol\ kg})$	84.21	30.05
$\mathbf{B}$	0.007796	0.0009558
$\mathbf{L_v}(\text{Å})$	0.8628	3.283

With all these parameters, it was possible to implement the model for this mixture. Using experimental VLE [45], excess volume and densities [46], and excess enthalpy [45] data, the adjustable parameters η_{ij} and ξ_{ij} were fitted, since with $\eta_{ij} = 1$ and $\xi_{ij} = 1$ the results are not accurate, as excepted due to the high deviation from the ideality of this mixture.

The fitting of the parameters η_{ij} and ξ_{ij} was made by first trying to fit the ξ_{ij} to have a good representation of the VLE and then the η_{ij} to have a good representation of the excess volume, but it was necessary to compromise the pressure in the VLE and have a better representation of the excess volume. The fitting as shown in Figure 19 was not possible once for lower ξ_{ij} values that represent an increase in the pressure, the VLE shows phase separation. It was chosen to have a better representation of the excess volume since the density is the most important properties that have an impact on all the other properties and because this mixture is known to have one of the highest excess volumes. So, it was necessary to increase the ξ_{ij} until no longer exists phase separation. At last, the best adjustable parameters providing the best representation not only of the excess volume but also the VLE and excess enthalpy are $\eta_{ij} = 1.012$ and $\xi_{ij} = 0.924$, and the results are presented in Figures 19-21.

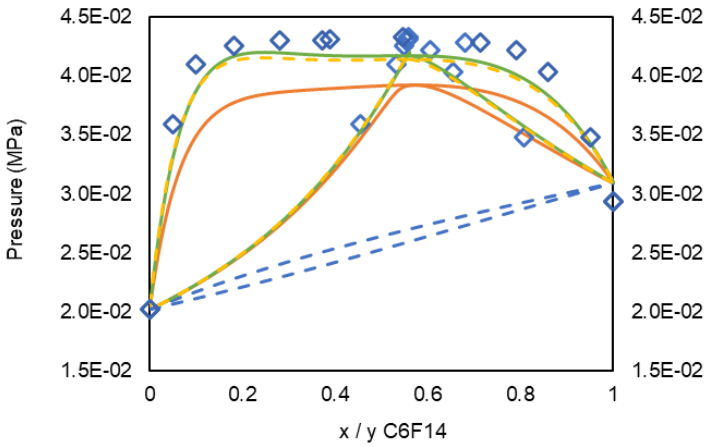

Figure 19. Isothermal VLE diagrams of Hexane with Perfluorohexane in over the composition of the fluorinated component at 298.15 K. Lines represent soft-SAFT calculations and symbols experimental data [45]. $(\eta_{ij} = 1; \xi_{ij} = 1)$, $(\eta_{ij} = 1; \xi_{ij} = 0.914)$, $(\eta_{ij} = 1.012; \xi_{ij} = 0.914)$ and $(\eta_{ij} = 1.012; \xi_{ij} = 0.924)$.

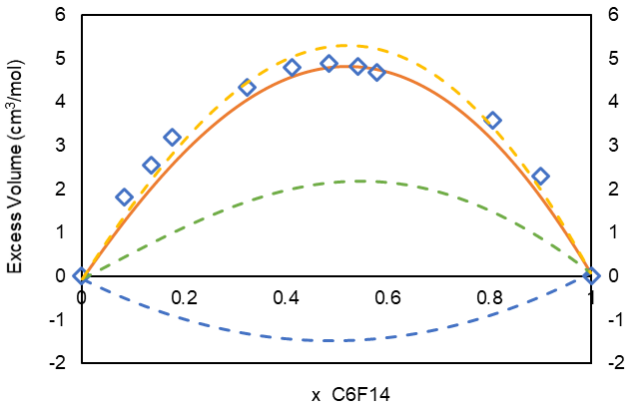

Figure 20. Excess Volume diagram of Hexane with Perfluorohexane over the composition of the fluorinated component at 298.15 K. Lines represent soft-SAFT calculations and symbols experimental data [46]. $(\eta_{ij} = 1; \xi_{ij} = 1)$, $(\eta_{ij} = 1; \xi_{ij} = 0.914)$, $(\eta_{ij} = 1.012; \xi_{ij} = 0.914)$ and $(\eta_{ij} = 1.012; \xi_{ij} = 0.924)$.

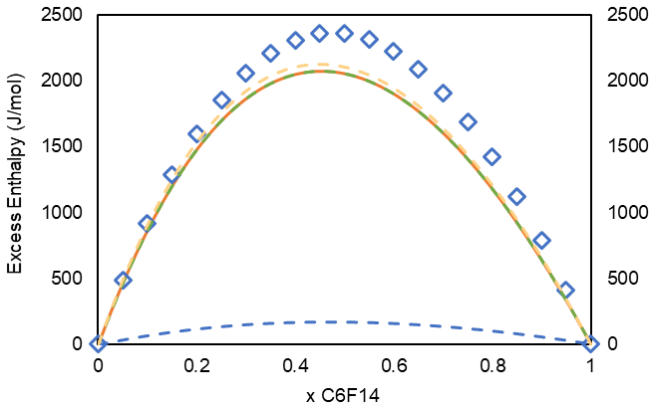

Figure 21. Excess Enthalpy diagram of Hexane with Perfluorohexane over the composition of the fluorinated component at 298.15 K. Lines represent soft-SAFT calculations and symbols experimental data [45]. $(\eta_{ij} = 1; \xi_{ij} = 1)$, $(\eta_{ij} = 1; \xi_{ij} = 0.914)$, $(\eta_{ij} = 1.012; \xi_{ij} = 0.914)$ and $(\eta_{ij} = 1.012; \xi_{ij} = 0.924)$.

The viscosity of the mixture was obtained by coupling soft-SAFT with FTV. With the mixing rules form Equation (67) to Equation (69), the results were obtained and exposed in Figure 22. The agreement with the experimental data from Morgado [44] is excellent.

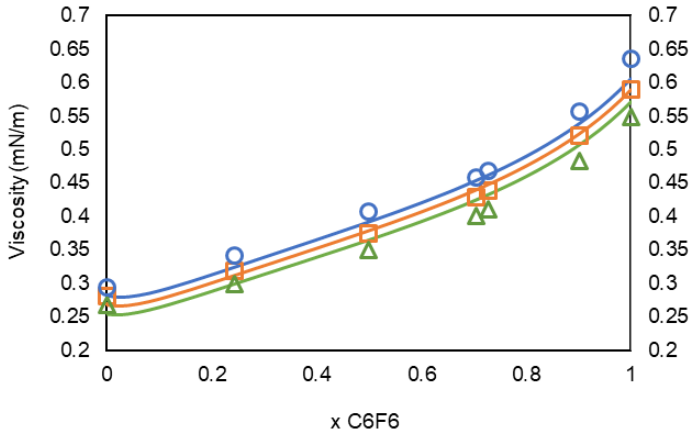

Figure 22. Viscosities for Hexane with Perfluorohexane over the composition of the fluorinated component at 0.1013 MPa. Solid lines represent soft-SAFT+FVT calculations and symbols experimental data [44]. ○ **293.15 K**, □ **303.15 K**, Δ **308.15 K**.

At last, for interface calculations, it was studied the surface tensions with different adjustable parameters for Equation (46) in order to have a good description of the surface tension when compared with the experimental data. Different articles were this experimental data available have different results like the one from Handa and Mukerjee [47] and Bowers *et al.* [7]. The results compared in Figure 23 are from reference [47]. A systematic study was performed changing the value of the β_{ij}, starting from ideal ($\beta_{ij} = 1$); the parameter that better describe the surface tension of this mixture is $\beta_{ij} = 0.4$ and the parameter that have a better agreement with the composition of the aneotrope is $\beta_{ij} = 0.8$.

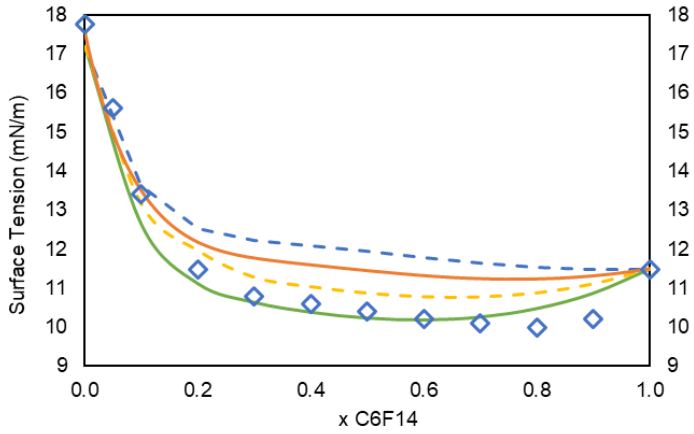

Figure 23. Surface tension for hexane with perfluorohexane over the composition of the fluorinated component at 298.15 K. Lines represents soft-SAFT+DGT calculations and symbols experimental data [47]. $\beta_{ij} = 1$, $\beta_{ij} = 0.8$, $\beta_{ij} = 0.6$ and $\beta_{ij} = 0.4$.

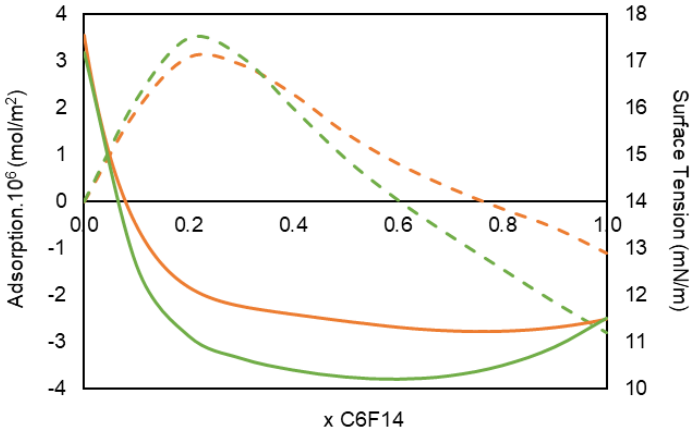

Figure 24. Surface tension (solid line) and adsorption (dashed line) for Hexane with Perfluorohexane over the composition of the fluorinated component at 298.15 K. $\beta_{ij} = 0.8$ and $\beta_{ij} = 0.4$.

In Figure 24 it is shown the adsorption of the mixture to the surface for $\beta_{ij} = 0.8$ and $\beta_{ij} = 0.4$. For concentrations less than 0.2 the Perfluorohexane migrate at a constant rate to the surface in order to reduce the surface tension, and then the rate slows down until a concentration of approximal 0.78 with a surface tension of 11.24 mN/m for $\beta_{ij} = 0.8$ and approximal 0.69 with a surface tension of 10.78 mN/m for $\beta_{ij} = 0.4$, at this point, hexane migrates to the surface, and the surface tension begins to increase. This turning point is called aneotrope and is a minimum in the surface tension. This minimum appears because, as shown with the high values of the excess enthalpy and volume, the two components of the mixture do not like to interact with each other. For that reason, in the interface, at aneotrope composition, they interact in such a way that the surface tension is less than the one from the component with the lowest value, in this case, the perfluorohexane.

6.2.3. Fluorinated with Hydrogenated Alcohols

All the parameters needed to describe the pure fluids are known, making it possible to proceed for the study of the mixtures. The mixtures are HFB with butanol, UFH with hexanol, and PDFO with decanol. The available experimental data for these mixtures is not vast, the densities, excess volumes of HFB with butanol and UFH with hexanol and molar volume of PDFO with decanol come from Morgado [6]. For the interface properties, the data available are the surface tension of each mixture at 298.15 K that is not published yet. At last, for the viscosities, the experimental data available is only for HFB with butanol and UFH with hexanol for a range of temperatures between 283.15 K and 353.15 K at atmospheric pressure from Costa [14]. There are also simulation results for the excess volume and enthalpy from Morgado [6] and Afonso [19].

The prediction of the excess enthalpies and volumes and VLE diagrams for the three mixtures was made using the same η_{ij} and ξ_{ij} as used for the hexane with perfluorohexane mixture ($\eta_{ij} = 0.012$ and $\xi_{ij} = 0.924$), in a transferable manner. However, now these mixtures have an OH group that brings an attractive side to the components, that for the hexane and perfluorohexane does not exist. For that reason, it is necessary to adjust the association parameter (α_{ij}^{HB}) for the experimental and simulation data of excess enthalpies, since the smallest change in the α_{ij}^{HB} have a considerable impact on energy. So, the excess enthalpies of the three mixtures with different α_{ij}^{HB} values are presented in Figure 25, Figure 26, and Figure 27, where soft-SAFT calculations are compared with available simulation and experimental data [6]. The dashed yellow line represents predictions from pure component parameters, while the other lines represent different sets of binary parameters, with η_{ij} and ξ_{ij} transferred from the hexane with perfluorohexane mixture when different than one.

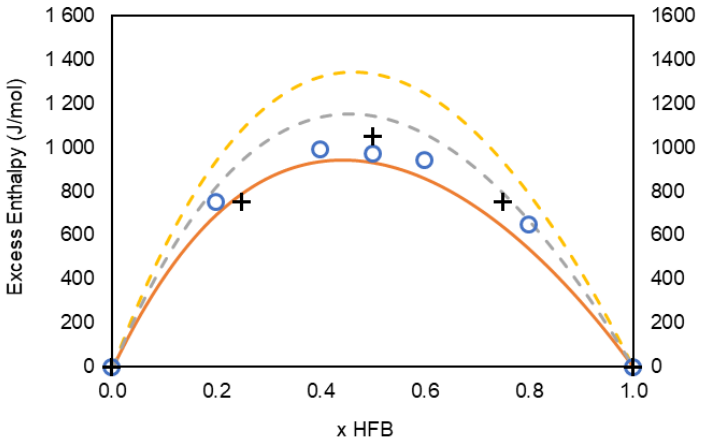

Figure 25. Excess Enthalpy for the HFB with Butanol mixture over the composition of HFB at 298.15 K. Lines represent soft-SAFT, open symbols the experimental data [6], and crosses simulation data [6]. Pure predictions $(\eta_{ij} = 1;\ \xi_{ij} = 1;\ \alpha_{ij}^{HB} = 1)$, $(\eta_{ij} = 1;\ \xi_{ij} = 0.914;\ \alpha_{ij}^{HB} = 1.01)$ and $(\eta_{ij} = 1.012;\ \xi_{ij} = 0.914;\ \alpha_{ij}^{HB} = 1.02)$.

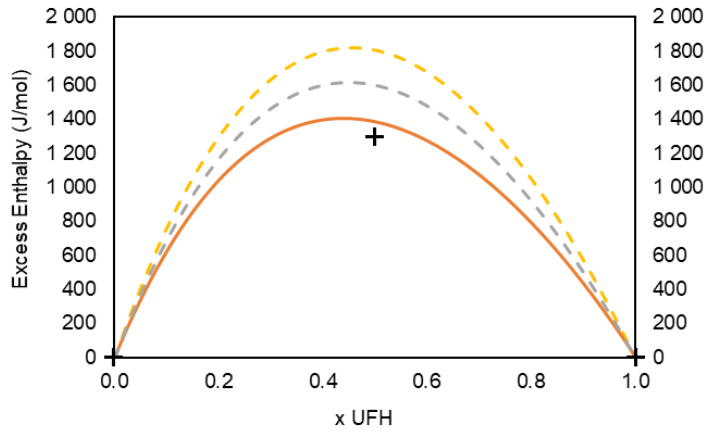

Figure 26. Excess Enthalpy for the UFH with Hexanol mixture over the composition of UFH at 298.15 K. Lines represent soft-SAFT and crosses simulation data [19]. $(\eta_{ij} = 1;\ \xi_{ij} = 1;\ \alpha_{ij}^{HB} = 1)$, $(\eta_{ij} = 1;\ \xi_{ij} = 0.914;\ \alpha_{ij}^{HB} = 1.01)$ and $(\eta_{ij} = 1.012;\ \xi_{ij} = 0.914;\ \alpha_{ij}^{HB} = 1.02)$.

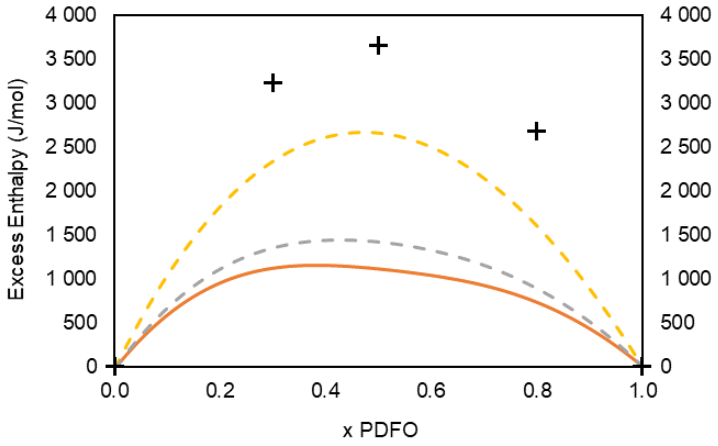

Figure 27. Excess Enthalpy for the PDFO with Decanol mixture over the composition of PDFO at 298.15 K. Lines represent soft-SAFT and crosses simulation data [19]. $(\eta_{ij} = 1;\ \xi_{ij} = 1;\ \alpha_{ij}^{HB} = 1)$, $(\eta_{ij} = 1;\ \xi_{ij} = 0.914;\ \alpha_{ij}^{HB} = 1.05)$ and $(\eta_{ij} = 1.012;\ \xi_{ij} = 0.914;\ \alpha_{ij}^{HB} = 1.06)$.

In order to have a proper fitting of α_{ij}^{HB} to have a correct model, it has necessary, like for the hexane with perfluorohexane mixture, to take into consideration the phase separation in the VLE diagrams. For the HFB with butanol and UFH with hexanol, it was possible to use the same α_{ij}^{HB} that describe all the properties, the best adjustable parameter value is $\alpha_{ij}^{HB} = 1.02$. For the PDFO with decanol mixture, the VLE diagram using $\alpha_{ij}^{HB} = 1.02$ shows phase separation, which does not exist experimentally, hence, it was necessary to fit this parameter to $\alpha_{ij}^{HB} = 1.06$. Unfortunately, this value does not provide a good agreement with the excess enthalpy predicted from the molecular simulations [6][19], but the results have already a significant impact.

The results for the VLE diagrams of the three mixtures are predictions since it does not exist experimental data to compare the results. However, in Figure 28, Figure 29, and Figure 30 is possible to see the different results with different α_{ij}^{HB} values to show the existence of phase separation for the UFH with hexanol and PDFO with decanol with lower α_{ij}^{HB} values.

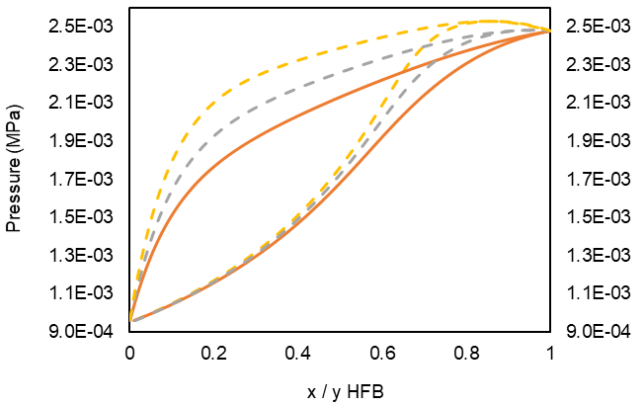

Figure 28. Isothermal VLE diagrams for HFB with Butanol over the composition of HFB at 298.15 K. Lines represent soft-SAFT calculations. $(\eta_{ij} = 1;\ \xi_{ij} = 1;\ \alpha_{ij}^{HB} = 1)$, $(\eta_{ij} = 1;\ \xi_{ij} = 0.914;\ \alpha_{ij}^{HB} = 1.01)$ and $(\eta_{ij} = 1.012;\ \xi_{ij} = 0.914;\ \alpha_{ij}^{HB} = 1.02)$.

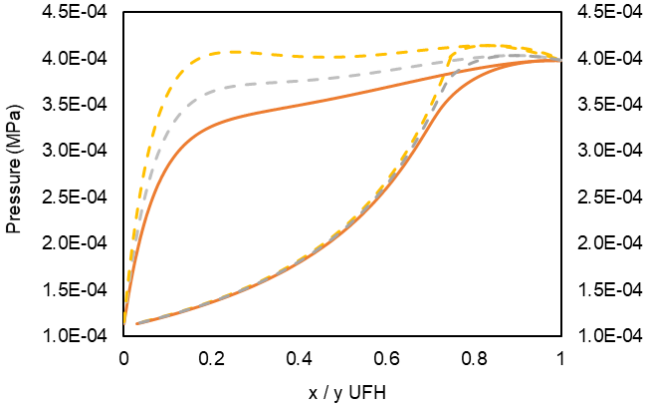

Figure 29. Isothermal VLE diagrams for UFH with Hexanol over the composition of UFH at 298.15 K. Lines represent soft-SAFT calculations. $(\eta_{ij} = 1;\ \xi_{ij} = 1;\ \alpha_{ij}^{HB} = 1)$, $(\eta_{ij} = 1;\ \xi_{ij} = 0.914;\ \alpha_{ij}^{HB} = 1.01)$ and $(\eta_{ij} = 1.012;\ \xi_{ij} = 0.914;\ \alpha_{ij}^{HB} = 1.02)$.

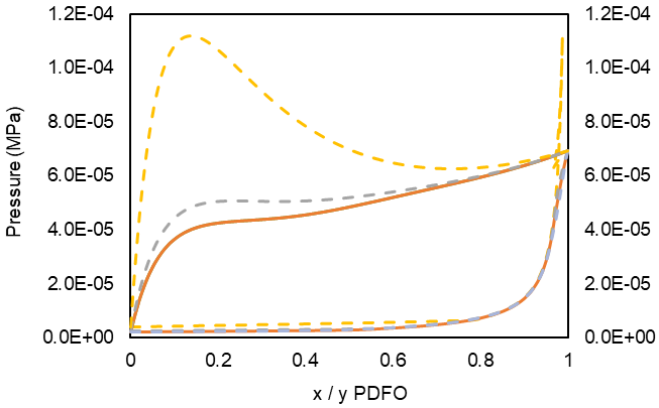

Figure 30. Isothermal VLE diagrams for PDFO with Decanol over the composition of PDFO at 298.15 K. Lines represent soft-SAFT calculations. $(\eta_{ij} = 1;\ \xi_{ij} = 1;\ \alpha_{ij}^{HB} = 1)$, $(\eta_{ij} = 1;\ \xi_{ij} = 0.914;\ \alpha_{ij}^{HB} = 1.05)$ and $(\eta_{ij} = 1.012;\ \xi_{ij} = 0.914;\ \alpha_{ij}^{HB} = 1.06)$.

The parameter α_{ij}^{HB} does not have a significant impact on the volume but only transferring the η_{ij} value from the hexane with perfluorohexane mixture, the results are great, as shown in Figure 31, Figure 32, and Figure 33. It is possible for the HFB with butanol and UFH with hexanol to compare the results from soft-SAFT with the experimental data, but for the PDFO with decanol mixture only exists simulation data. Although, the agreement of the simulation data for the other mixtures is excellent.

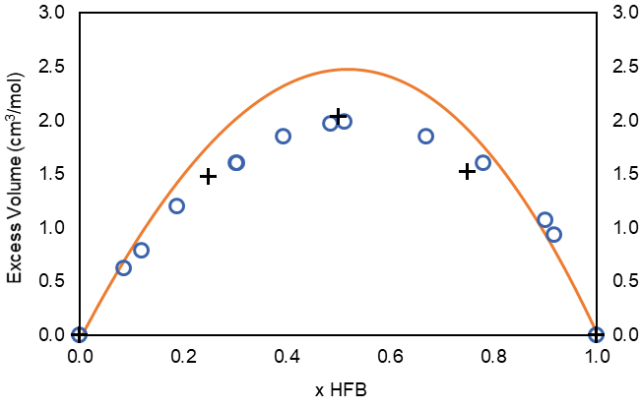

Figure 31. Excess Volume for the HFB with Butanol mixture over the composition of HFB at 298.15 K. Lines represent soft-SAFT, open symbols the experimental data [6], and crosses simulation data [6].

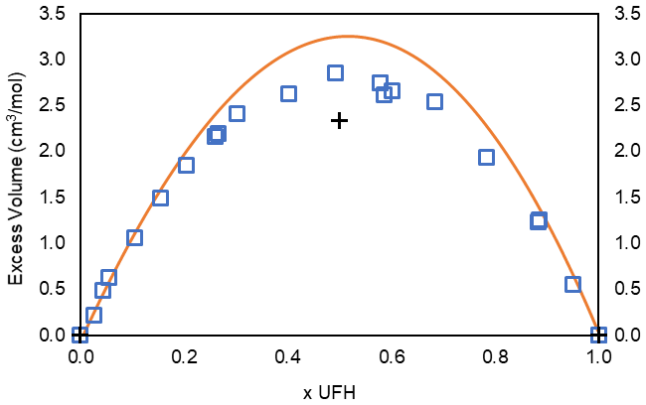

Figure 32. Excess Volume for the UFH with Hexanol mixture over the composition of UFH at 298.15 K. Lines represent soft-SAFT, open symbols the experimental data [6], and crosses simulation data [19].

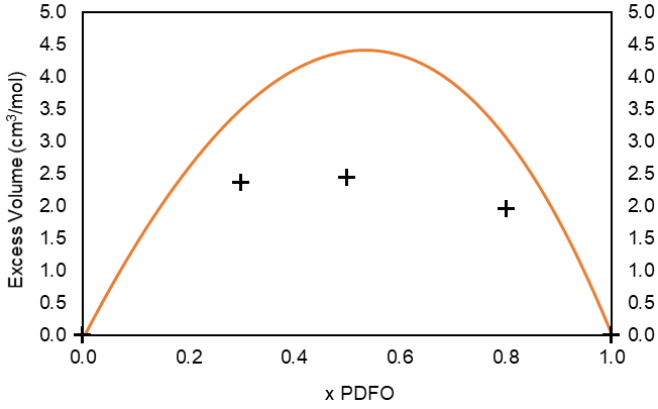

Figure 33. Excess Volume for the PDFO with Decanol mixture over the composition of PDFO at 298.15 K. Lines represent soft-SAFT, open symbols the experimental data, and crosses simulation data [19].

By analyzing the excess volume, it is possible to observe that the model captures the curve tendencies with success for the three mixtures and that the agreement for the HFB with butanol and UFH with hexanol is excellent for both experimental [6] and simulation data [6][19]. However, the agreement for PDFO with decanol is not high when compared with the simulation data. For these mixtures, as said, the adjustable parameters η_{ij} and ξ_{ij} are transferred from the study of hexane with perfluorohexane being the goal only change the association part. By doing this the binary parameter η_{ij} is the one that could be adjected to give good agreement with the experimental data for the excess volume, since this parameter has a substantial impact on this property. However, one goal of this work is to see if the same parameters can work for all the family mixtures, as we are searching for trends that may be hidden if all parameters are fitted, and we try to build models as predictive as possible.

The excess volumes are positive because of the way that the two components of every mixture, interact with each other since, as known, the two components do not interact well in the hydrophobic parts. However, the OH group gives to these mixtures an association that brings complexity to the way that the molecules prefer to arrange in the bulk. Furthermore, because of that and for bigger hydrophobic groups like for PDFO with decanol, the excess volumes are higher, showing the massive impact of this group.

For the excess enthalpies, soft-SAFT gives accurate results for the HFB with butanol and UFH with hexanol when compared with the simulations data, for the PDFO with decanol the agreement is not tremendous but changing only the α_{ij}^{HB} the results have already a significant impact. Still, the inexistence of experimental data gives to these results a predictive character, to be assessed when experimental data are available.

The excess enthalpy predicted for these mixtures are positive, and as shown by Morgado [6] for all mixtures of this family, the Coulomb interactions, that account for hydrogen-bond interactions, are negative, and the dispersive interactions are positive, although the impact of each interaction is different for each mixture. For mixtures with less carbon number as TFE with ethanol, the impact of the hydrogen-bond is more significant than the dispersive forces, so the excess global enthalpies are negative. However, for mixtures with higher carbon numbers like the mixtures studied in this work, the dispersive part is more positive and the Coulomb less negative, and for that reason, the excess enthalpies are positive.

6.2.3.1. Viscosities

The next step was the calculation of the viscosities. The experimental data available for these mixtures were obtained by Costa [14] and is only for HFB with Butanol and UFH with Hexanol. The experimental values are at atmospheric pressure, and for a temperature range between 283 and 353 K. Using Equation (66) and the mixing roles proposed, the results of the viscosities, for all the three mixtures, are exposed in Figure 34, Figure 35, Figure 36 and Figure 37.

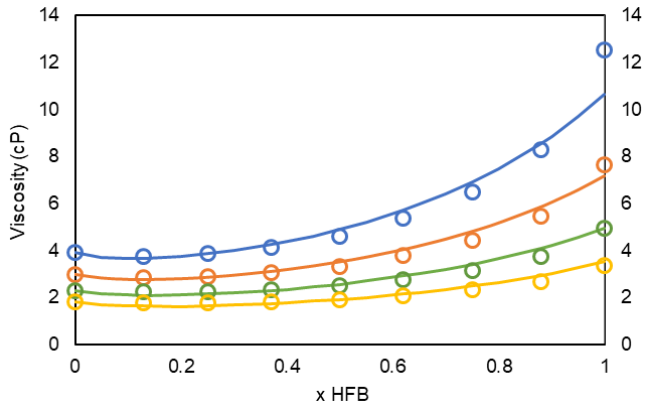

Figure 34. Viscosities for HFB with Butanol over the composition of the fluorinated component at 0.1013 MPa. Solid lines represent soft-SAFT+FVT calculations and symbols experimental data [14]. **283.15 K**, **293.15 K**, **303.15 K**, **313.15 K**.

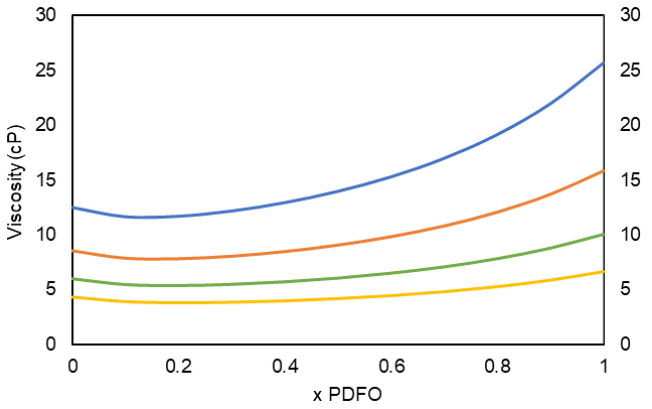

Figure 35. Viscosities for PDFO with Decanol over the composition of the fluorinated component at 0.1013 MPa. Solid lines represent soft-SAFT+FVT calculations. **283.15 K**, **293.15 K**, **303.15 K**, **313.15 K**.

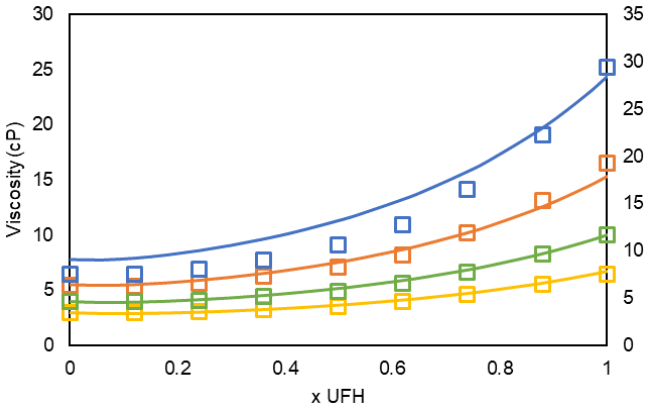

Figure 36. Viscosities for UFH with Hexanol over the composition of the fluorinated component at 0.1013 MPa. Solid lines represent soft-SAFT+FVT calculations and symbols experimental data [14]. **283.15 K**, **293.15 K**, **303.15 K**, **313.15 K**.

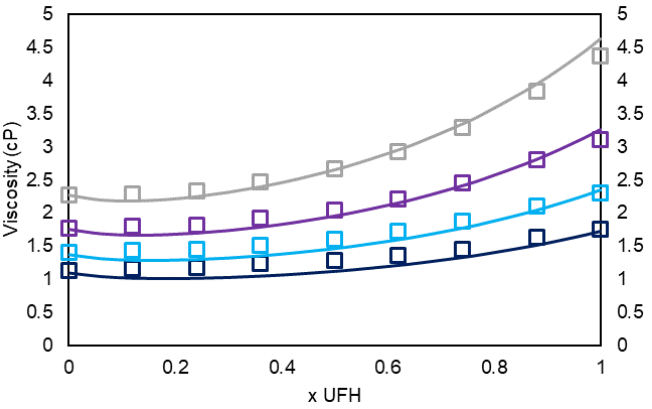

Figure 37. Viscosities for UFH with Hexanol over the composition of the fluorinated component at 0.1013 MPa. Solid lines represent soft-SAFT+FVT calculations and symbols experimental data [14]. **323.15 K**, **333.15 K**, **343.15 K**, **353.15 K.**

Analyzing the results is possible to see that the agreement between the experimental data and soft-SAFT with FTV results are, overall, excellent for HFB with butanol and UFH with hexanol. The results for PDFO with decanol are pure predictions, and the parameters of the pure components used come from correlations 84, 85, and 86 for decanol and 70, 71, and 72 for PDFO. The most considerable deviations from the experimental data appear at 283.15 K at higher compositions of the fluorinated components. All the viscosities have negative deviations for the ideality, and this occurs because of the way that the hydrophobic part of the molecules behave between unlike molecules, and this represents a more fluid flow than the pure components case. As expected from Equation (66), the temperature has a significant impact on the viscosity since in higher temperatures exists an increase in the molecular interchange as molecules move faster.

6.2.3.2. Surface Tensions

The aneotrope is the existence of a minimum in the surface tension and is expected for these mixtures to have one, as shown in the experimental data. For interface calculations, it is necessary one more adjustable parameter (β_{ij}), and it was fitted comparing the experimental data with the results form soft-SAFT coupled with DGT. Without any adjust ($\beta_{ij} = 1$, which direct combination of the influence parameter of the two pure components), the results already have the deviations from linearity, as expected. However, the expected aneotrope does not appear. For this reason, and as shown for similar studies for these family mixtures [11], it is needed to use the adjustable parameter in order to obtain good results. For the three mixtures the better β_{ij} to describe the surface tensions is 0.8.

In Figure 38, Figure 39 and Figure 40 the results are exposed for the surface tension using soft-SAFT with DGT for $\beta_{ij} = 1$, $\beta_{ij} = 0.9$, and $\beta_{ij} = 0.8$.

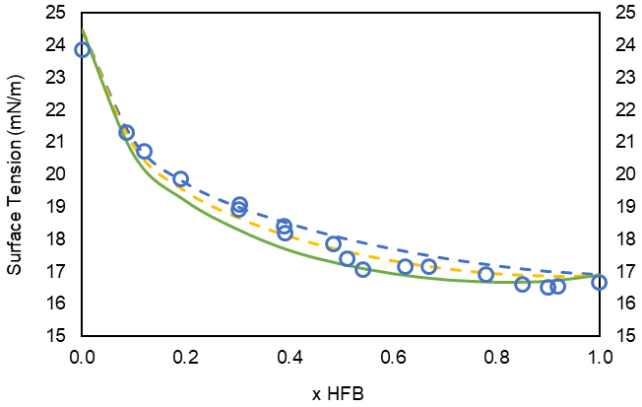

Figure 38. Surface tension for HFB with Butanol over the composition of the fluorinated component at 298.15 K. Lines represents soft-SAFT + DGT, and symbols represent experimental data. $(\beta_{ij} = 1)$, $(\beta_{ij} = 0.9)$, and $(\beta_{ij} = 0.8)$.

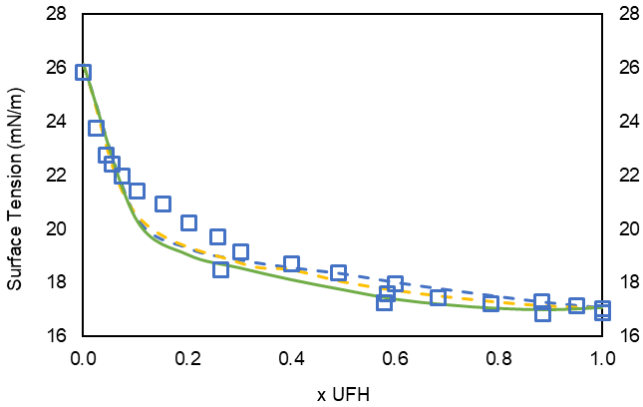

Figure 39. Surface tension for UFH with Hexanol over the composition of the fluorinated component at 298.15 K. Lines represents soft-SAFT + DGT, and symbols represent experimental data. $(\beta_{ij} = 1)$, $(\beta_{ij} = 0.9)$, and $(\beta_{ij} = 0.8)$.

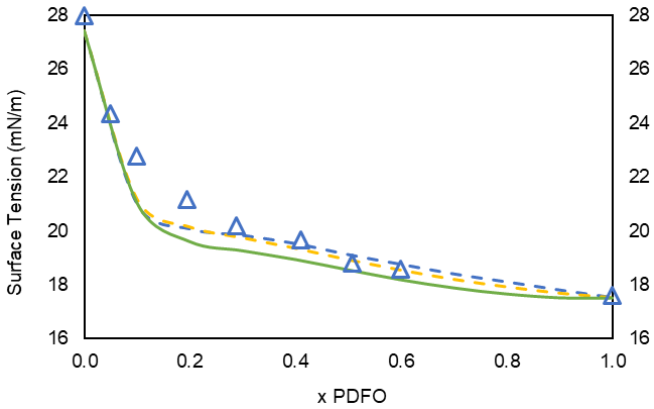

Figure 40. Surface tension for PDFO with Decanol over the composition of the fluorinated component at 298.15 K. Lines represents soft-SAFT + DGT, and symbols represent experimental data. $(\beta_{ij} = 1)$, $(\beta_{ij} = 0.9)$, and $(\beta_{ij} = 0.8)$.

As represented in Figure 38, Figure 39 and Figure 40, the model with $\beta_{ij} = 0.8$ predicts with good accuracy, the surface tension curves of all the mixtures. With $\beta_{ij} = 0.9$ the HFB with butanol mixture has already aneotrope. However, the $\beta_{ij} = 0.8$ represents better the aneotrope, and it is possible to have the same parameter for the three mixtures.

The model predicts the presence of an aneotrope in all mixtures, and the composition and surface tension of the aneotrope is showed in Table 6 as the experimental values expected. The experimental values of the surface tension of PDFO with decanol were not possible to obtain since, at compositions higher than 0.6, the mixture solidifies at 298.15 K. So, the values given by the model are predictions if the mixture at that temperature and right conditions was liquid.

Table 6. Experimental and soft-SAFT with DGT calculations of the aneotrope compositions and surface tension.

Mixture	Experimental		soft-SAFT + DGT	
	x	ST (mN/m)	x	ST (mN/m)
HFB + Butanol	0.90	16.52	0.82	16.84
UFH + Hexanol	0.885	16.85	0.90	16.98
PDFO + Decanol	-	-	0.98	17.52

6.2.3.3. Density Profiles

In order to calculate the surface tension, DGT predicts the density profiles for each concentration. The aneotrope came from the unfavored interactions between molecules present at the surface and in order to take more conclusions about what occurred at the surface, it is important to analyze the density profiles for compositions before (Figure 41), after (Figure 42) and at the aneotrope (Figure 43). These calculations were made using $\beta_{ij} = 0.8$.

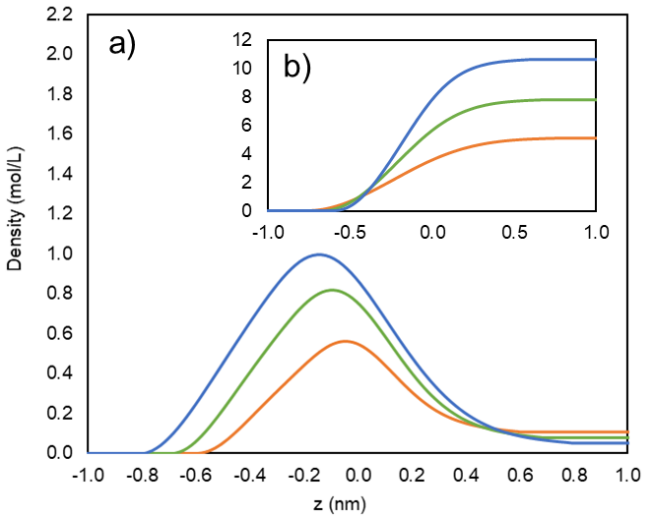

Figure 41. Density profiles of the fluorinated alcohols mixtures with hydrogenated alcohols for a composition of 0.01 relative to the fluorinated alcohol. a) Density profile of the fluorinated alcohols. b) Density profile of the hydrogenated alcohols. Solid lines represent soft-SAFT + DGT calculations. **HFB + ButOH**, **UFH + HexOH** and **PDFO + DecOH**.

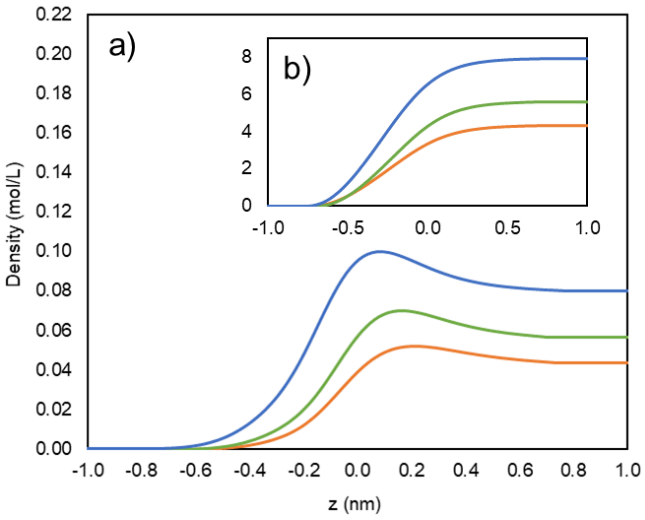

Figure 42. Density profiles of the fluorinated alcohols mixtures with hydrogenated alcohols for a composition of 0.99 relative to the fluorinated alcohol. a) Density profile of the hydrogenated alcohols. b) Density profile of the fluorinated alcohols. Solid lines represent soft-SAFT + DGT calculations. **HFB + ButOH**, **UFH + HexOH** and **PDFO + DecOH**.

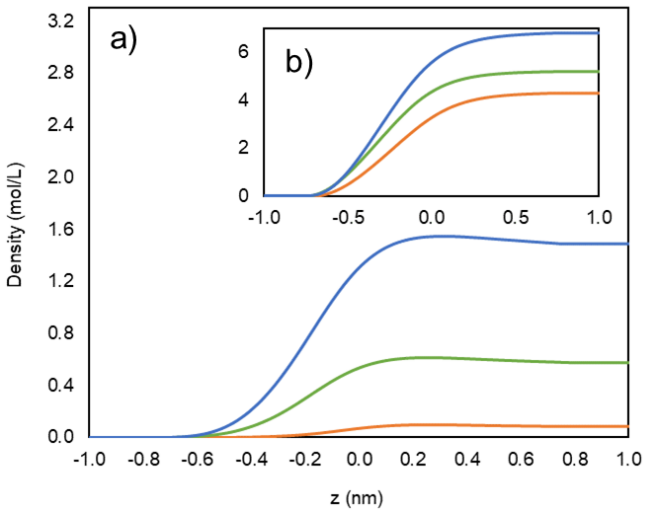

Figure 43. Density profiles of the fluorinated alcohols mixtures with hydrogenated alcohols at aneotrope composition relative to the fluorinated alcohol. a) Density profile of the hydrogenated alcohols. b) Density profile of the fluorinated alcohols. Solid lines represent soft-SAFT + DGT calculations. **HFB + ButOH**, **UFH + HexOH** and **PDFO + DecOH**.

Before aneotrope composition in Figure 41, it is possible to conclude with the density profiles that the fluorinated alcohols are strongly adsorbed to the interface while the density of the hydrogenated alcohols at the interface is constant — culminating in a decreasing of the surface tension, due to the amphophilic behavior inherent of the surfactants. However, after the aneotrope composition, in Figure 42, it is the hydrogenated alcohols that migrate to the interface, and this causes a rise in the surface tension. In Figure 43, at aneotrope compositions, it is possible to see small adsorption of the hydrogenated alcohols, since, at this composition, the relative adsorption inverts from one to another component, so at the exact aneotrope composition neither the fluorinated alcohols or the hydrogenated alcohols migrate to the surface.

6.2.3.4. Adsorption at the interface

To have further conclusions and a better idea of what could occur at the interface is crucial to understand also the adsorption in this region. Once more, the adsorption was calculated using Equation (51), and the following figures show the adsorption of each mixture relative to the composition of the fluorinated alcohol component with $\beta_{ij} = 0.8$.

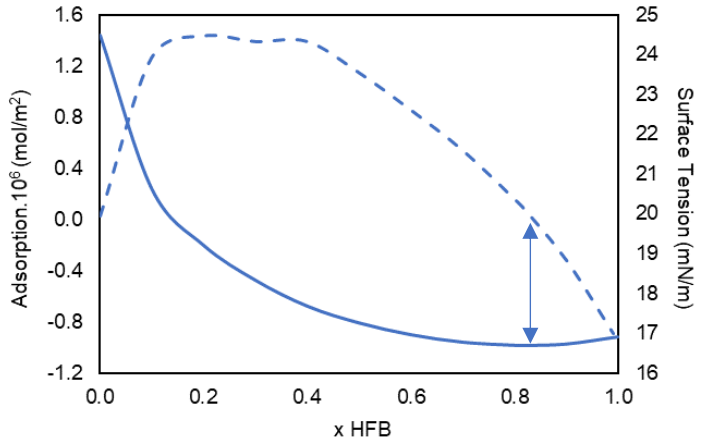

Figure 44. Surface tension (solid line) and adsorption (dashed line) of HFB + ButOH mixture. The two sides arrow represent the aneotrope.

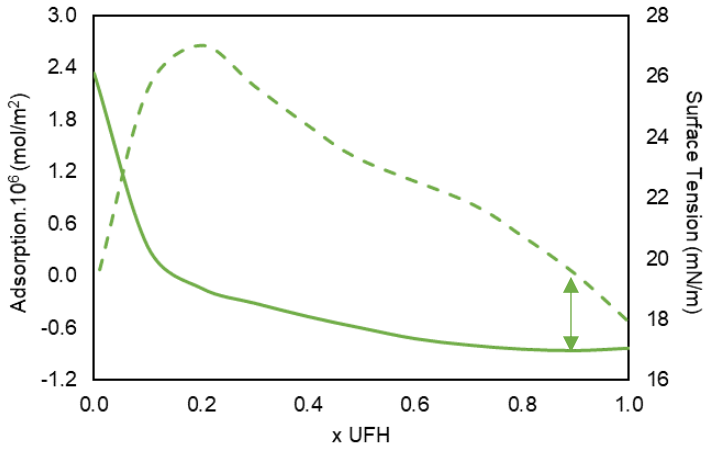

Figure 45. Surface tension (solid line) and adsorption (dashed line) of UFH + HexOH mixture. The two sides arrow represent the aneotrope.

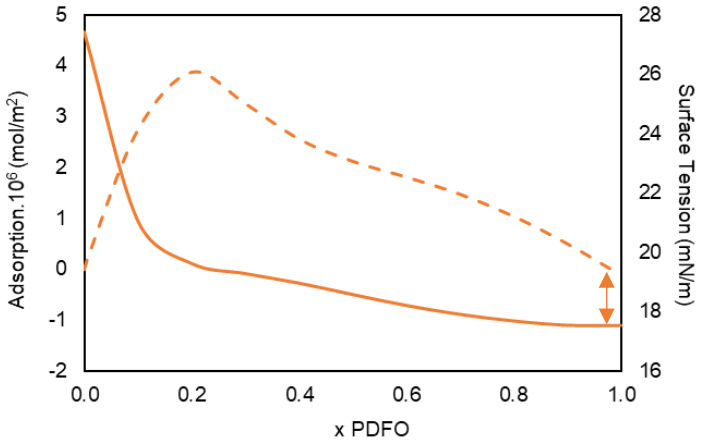

Figure 46. Surface tension (solid line) and adsorption (dashed line) of PDFO + DecOH mixture. The two sides arrow represent the aneotrope.

In Figure 44, Figure 45 and Figure 46, one observes that the absorption of the fluorinated alcohols increases almost linearly until around composition of 0.2, which represents a migration of the surfactants to the interface to reduce the surface tension. At this first state for mixtures with heavier components, more surfactants migrate to the surface, and this is because heavier surfactants have a more significant impact on the decreasing of the surface tension.

For the HFB with butanol mixture exist a baseline, and at these compositions, the adsorption is almost constant, so the concentration at the surface is continual. Then at compositions higher than 0.5 for HFB with butanol and compositions higher than 0.2 for UFH with hexanol and PDFO with decanol, the adsorption of the surfactants to the surface decrease until a composition where the adsorption is zero. So, in order to reduce the surface, tension is needed fewer surfactants at the interface. At aneotrope composition, there is no adsorption, and the way that the molecules organize at the surface is the one that allowed a minimum in the surface tension even less than the surface tension of the surfactants. After the aneotrope composition, the hydrogenated alcohols travel to the interface, increasing the surface tension.

A hypothesis that could explain this behavior at the surface is the phase separation between the two components at the surface, so the adsorption at the beginning of the fluorinated alcohol is much higher, meaning that the surfactants are migrating to the surface in order to decrees de surface tension. Around the composition of 0.2, the phase separation begins to occur, and the adsorption drops until a specific concentration, and this is the technique that the molecules prefer to impact at the surface in order to reduce the surface tension.

7. Conclusions

This work has been devoted to the study of thermodynamic, viscosities and interfacial properties of fluorinated with hydrogenated alcohols mixtures using the soft-SAFT equation of state coupled with other theories, and results compared to available experimental and molecular simulation data.

The viscosity parameters obtain by using soft-SAFT coupled with FVT for the fluorinated alcohols family, from TFE to TRFH, describe well the pure components having a good agreement with the experimental data, especially for higher temperatures. Using a correlation to describe the tendency of each parameter in the family with their molecular weight allows predicting the parameters for other heavier members of the family. These parameters and correlations made possible not only to calculate first and second-order derivatives and interfacial properties with the parameters fitted in previous works [11] but also to calculate transport properties of both pure and mixtures of fluorinated alcohols.

For the mixtures of HFB with butanol, UFH with hexanol, and PDFO with decanol calculations, the VLE diagrams were predicted using soft-SAFT since experimental data for these mixtures was not available. soft-SAFT captured the excess volumes and excess enthalpies tendency with excellent agreement when compared with the experimental and simulation data available. However, for the PDFO with decanol, the agreement is not exceptional, this could be because this mixture solidify for concentrations of PDFO higher than 0.6 and as concluded by Afonso [19] in this mixture the fluorinated and hydrogenated chains are already so large that the hydrogen bonds between different components do not exist, meaning that the components no longer have an attraction.

Using the binary parameters transferred from hexane with perfluorohexane ($\eta_{ij} = 1.012$ and $\xi_{ij} = 0.924$) the fitting of the association parameter (α_{ij}^{HB}) provided an excellent description of the properties of the mixtures between the alcohols. For the HFB with butanol and UFH with hexanol mixtures the α_{ij}^{HB} needed was 1.02, and for the PDFO with decanol mixture was 1.06. Globally this strategy works very well for all the properties investigated, giving meaningful and robust results.

The viscosities of the binary mixtures HFB with Butanol and UFH with Hexanol were successfully captured, being more accurate for higher temperatures as expected relative to the pure components.

At last, the interfacial properties of all the three mixtures were captured with success, using a value of the β_{ij} parameter equal to 0.8 to describe all mixtures. The results of surface tension, density profiles, and preferential adsorptions allow to obtain molecular insights into the non-ideal surface behavior of these distinct mixtures.

For future work, to better understand what happens at the surface is crucial, regarding these mixtures, to do molecular simulations at the interface. It is also crucial to do more experimental studies about VLE and derivative properties in order to corroborate the model calculations for these properties. One more essential thing is to study deeper the PDFO with decanol mixture and heavier mixtures in order to understand the impact of the chain length and the interaction within these mixtures.

8. References

[1]. F. J. Blas, L. F. Vega, Prediction of Binary and Ternary Diagrams using the Statistical Associating Fluid Theory (SAFT) Equation of State. Ind. Eng. Chem. Res. **1998**, 37, 660.

[2]. F. J. Blas, L. F. Vega, Thermodynamic Behavior of Homonuclear and Heteronuclear Lennard-Jones Chains with Association Sites from Simulation and Theory. Mol. Phys. **1997**,92, 135.

[3]. I. G. Economou, Statistical Associating Fluid Theory: A Successful Model for the Calculation of Thermodynamic and Phase Equilibrium Properties of Complex Fluid Mixtures, Ind. Eng. Chem. Res. **2002,** 41, 953-962.

[4]. C. Duce, M. Tinè, L. Lepori, E. Matteoli. VLE and LLE of perfluoroalkane + alkane mixtures. Fluid Phase Equilibria 2002, 199, 197–212.

[5]. L. F. Martins, L. A. Pereira, G. M. Silva, J. R. Ascenso, P. Morgado, J. P. Ramalho, E. J. Filipe. Fluorinated surfactants in solution: Diffusion coefficients of fluorinated alcohols in water. Fluid Phase Equilibria, **2015**, 407,322-333.

[6]. P. Morgado, A. R. Garcia, L. M. Ilharco, J. Marcos, M. Anastácio, L. F. G. Martins, E. J. M. Filipe. Liquid Mixtures Involving Hydrogenated and Fluorinated Alcohols: Thermodynamics, Spectroscopy, and Simulation. The Journal of Physical Chemistry B, **2016**, pageacs.jpcb.6b04297.

[7]. J. Bowers, I. McLure, R. Whitfield, and A. Burgess, Surface Composition Studies on (n-Hexane + Perfluoro-n-hexane) by Specular Neutron Reflection, Langmuir **1997**, 137, 2167-2170.

[8]. I. Shuklov, N. Dubrovina, A. Borner, Fluorinated alcohols as solvents, co-solvents, and additives in homogeneous catalysis, SYNTHESIS **2007**, 19, 2925–2943.

[9]. P. D. Mobley, A. V. Rayer, J. Tanthana, T. R. Gohndrone, M. Soukri, L. J. Coleman, and M. Lail. CO2 Capture Using Fluorinated Hydrophobic Solvents. Industrial and Engineering Chemistry Research, **2017**, 56(41): 11958-11966.

[10]. J. Justino, Thermodynamic and Interfacial properties of hydrogenated and fluorinated alcohols mixtures: a molecular modeling approach, MSc. Thesis, IST Lisbon. **2018**.

[11]. G. M. C. Silva, J. Justino, P. Morgado, J. Afonso, M. Leitão, M. Teixeira, L. M. C. Pereira, LF. Vega, E. J. M. Filipe, Throughout characterization of surface tension of highly fluorinated alcohols: experimental, simulation and soft-SAFT-DGT modeling, J. Molec. Liquids, accepted (2019).

[12]. J. Salgado, T. Regueira, L. Luís, J. Vijande, J. Fernández, J. Carcía, Density, and viscosity of three (2,2,2-trifluoroethanol +1-butyl-3-methylimidazolium) ionic liquid binary systems, J. Chem. Thermodynamics, **2014**, 70, 101-110.

[13]. R. Palepu, J. Clarke, VISCOSITIES, AND DENSITIES OF 2,2,2-TRIFLUOROETI-IANOL + WATER AT VARIOUS TEMPERATURES, Thermochemical Acta, **1989**, 156, 359-363.

[14]. M. Costa, Property Data, and Phase Equilibria for the Design of Chemical Processes involving Carbon Dioxide, MSc. Thesis, IST Lisbon. **2017**.

[15]. S.K. Chaudhari, K.R. Patil, J. Allepús, A. Coronas, Measurement of the vapor pressure of 2,2,2-trifluoroethanol and tetraethylene glycol dimethyl ether by static method, Fluid Phase Equilib. **1995**, 108, 159–165.

[16]. P. Sauermann, K. Holzapfel, J. Oprzynski, J. Nixdorf, F. Kohler, Thermodynamic properties of saturated and compressed liquid 2,2,2-trifluoroethanol, Fluid Phase Equilib. **1993**, 84, 165–182.

[17]. G.M.C. Silva, P. Morgado, J.D. Haley, V.M.T. Montoya, C. McCabe, L.F.G. Martins, E.J.M. Filipe, Vapor pressure and liquid density of fluorinated alcohols: Experimental, simulation and GC-SAFT-VR predictions, Fluid Phase Equilib. **2016**, 425, 297–304.

[18]. J.C.S. Costa, M. Fulem, B. Schröder, J.A.P. Coutinho, M.J.S. Monte, L.M.N.B.F. Santos, Evidence of an odd-even effect on the thermodynamic parameters of odd fluorotelomer alcohols, J. Chem. Thermodyn. **2012**, 54, 171–178.

[19]. J. Afonso, Transport properties of fluorinated surfactants: viscosity and diffusion of mixtures involving fluorinated alcohols, MSc. Thesis, IST Lisbon. **2018**.

[20]. G.W. Chapman, Prediction of The Thermodynamic Properties of Associating Lennard-Jones Fluids: Theory and Simulation, J. Chem. Phys. **1990a**, 49, 2777.

[21]. G. Jackson, G. W. Chapman, K. E. Gubbins, Phase Equilibria of Associating Fluids Spherical Molecules with Multiple Bonding Sites. Mol. Phys. **1988**, 65, 1.

[22]. M. Nieves, G. Amparo, G. George, J. Andrew, N. Burgess, Predicting the high-pressure phase equilibria of binary aqueous solutions of 1-butanol, nbutoxyethanol and n-decylpentaoxyethylene ether (C10E5) using the SAFT-HS approach. Mol. Phys. **1998**, 93, 57-71.

[23]. Y. Peng, K.D. Goff, M.C. dos Ramos, C. McCabe, Developing a predictive group-contribution-based SAFT-VR equation of state, Fluid Phase Equilib. 277 (2009) 131–144. doi:10.1016/j.fluid.2008.11.008.

[24]. J. K. Johnson, J. Zollweg, K. Gubbins, The Lennard-Jones Equation of State Revisited. Mol. Phys. **1993**, 78, 591.

[25]. V. Papaioannou, T. Lafitte, C. Avendaño, C.S. Adjiman, G. Jackson, E.A. Müller, A. Galindo, Group contribution methodology based on the statistical associating fluid theory for heteronuclear molecules formed from Mie segments, J. Chem. Phys. **2014**, 140.

[26]. P. Atkins and J. Paula (**2006**). PHYSICAL CHEMISTRY. Eighth Edition, W.H Freeman and Company, New York.

[27]. Available in: https://www.studyorgo.com/blog/how-do-you-to-tell-when-a-hydrogen-bond-will-occur/. Access in: 10/09/2019.

[28]. J. M. Smith, H. C. Van Ness, M. M. Abbott, (**2005**) Introduction to Chemical Engineering Thermodynamics. Seventh Edition, Mc Graw Hill International Edition, New York.

[29]. F Llovell, LF Vega. Prediction of thermodynamic derivative properties of pure fluids through the soft-SAFT equation of state. J. Phys. Chem. B. **2006**, 110 (23), 11427-11437.

[30]. O. Vilaseca, L.F. Vega, Direct calculation of interfacial properties of fluids close to the critical region by a molecular-based equation of state, Fluid Phase Equilib. **2011**, 360, 4–14.

[31]. A. Mejía, J. Pàmies, D. Duque, H. Segura, L. F. Vega, Phase and interface behaviors in type-I and type-V Lennard-Jones mixtures: Theory and simulations, J. Chem. Phys. **2005**, 123, 034505.

[32]. N. Mac Dowell, F. Llovell, N. Sun, J. P. Hallett, A. George, P. A. Hunt, T. Welton, B. A. Simmons, and L. F. Vega, New Experimental Density Data and Soft-SAFT Models of Alkylimidazolium ([CnC1im]+) Chloride (Cl−), Methylsulfate ([MeSO4]−), and Dimethylphosphate ([Me2PO4]−) Based Ionic Liquids, J. Phys. Chem. B, **2014**, 118, 6206−622.

[33]. A. Adamson and A. Gast, Physical Chemistry of Surfaces, **1997**, Sixth Edition, Wiley-Interscience Publication, New York.

[34]. J. W. Cahn, J. E. Hilliard, Free Energy of a Nonuniform System. I. Interfacial Free Energy, J. Chem. Phys. **1958,** 28, 258.

[35]. J. C. Pàmies, Bulk and interfacial properties of chain fluids: a molecular modeling approach, Thesis. **2004**. http://www.tdx.cat/handle/10803/8522.

[36]. F. Llovell, R.M. Marcos, L.F. Vega, Free-volume-theory coupled with soft-SAFT for viscosity calculations: comparison with molecular simulation and experimental data, J.Phys. Chem. B., **2013**, 117, 8159–8171.

[37]. F. Llovell, R.M. Marcos, L.F. Vega, Transport properties of mixtures by the soft-SAFT + free-volume theory: application to mixtures of n-alkanes and hydrofluorocarbons, J. Phys. Chem. B. **2013**, 117, 5195–5205

[38]. F. Llovell, O. Vilaseca, N. Jung, L.F. Vega, Water + 1-alkanol systems: Modeling the phase, interface and viscosity properties, Fluid Phase Equilib. **2013**, 360, 367–378.

[39]. E. Cané, F. Llovell, L. F. Vega, Accurate viscosity predictions of linear polymers from n-alkanes data, Journal of Molecular Liquids, **2017**, 243, 115–123.

[40]. D. Viswanath, T. Ghosh, D. Prasad, N. Dutt, and K. Rani. Viscosity, of Liquids. Theory, Estimation, Experimental, and Data, **2017**, Springer, Dordrecht.

[41]. A. Allal, M. Moha-Ouchane, C Boned, A New Free Volume Model for Dynamic Viscosity and Density of Dense Fluids Versus Pressure and Temperature. Phys. Chem. Liq. **2001**, 39, 1−30.

[42]. A. Allal, C. Boned, A. Baylaucq, Free-Volume Viscosity Model for Fluids in the Dense and Gaseous States. Phys. Rev. E., **2001**, 64, 011203.

[43]. A.M.A. Dias, F. Llovell, J.A.P. Coutinho, I.M. Marrucho, L.F. Vega. Thermodynamic characterization of pure perfluoroalkanes, including interfacial and second-order derivative properties, using the crossover soft-SAFT EoS. Fluid Phase Equilibria **2009**, 286, 134–143.

[44]. P. Morgado, J. Blackb, J. Lewis, C. Iacovella, C. McCabe, L. Martins, E. Filipe. Viscosity of liquid systems involving hydrogenated and fluorinated substances: Liquid mixtures of (hexane + perfluorohexane) Fluid Phase Equilibria **2013**, 358, 161–165.

[45]. R. D. Dunlap, R. G. Bedford, J. C. Woodbrey, and S. D. Furrow. Liquid-Vapor Equilibrium for the System: Perfluoron-hexanen-Hexane. J. Am. Chem. Soc.**1959**, 8112, 2927-2930.

[46]. R. Bedford and R. Dunlap**.** Solubilities and Volume Changes Attending Mixing for the System: Perfluoro-n-hexane-n-Hexane. J. Am. Chem. Soc.**1958**, 802, 282-285.

[47]. T. Handa and P. Mukerjee, Surface tensions of nonideal mixtures of fluorocarbons and hydrocarbons and their interfacial tensions against water, J. Phys. Chem. **1981,** 8525, 3916-3920.

9. Appendix

9.1. Appendix A

For the fluorinated alcohols family, the correlations are:

$$m = 0.00473M_W + 1.28 \quad (73)$$

$$m\sigma^3 = 0.779M_W + 22.28 \quad (74)$$

$$m\varepsilon = 1.64M_W + 205.41 \quad (75)$$

$$c = 6.19 \times 10^{-24}{M_W}^2 - 5.44 \times 10^{-22}M_W + 8.92 \times 10^{-20} \quad (76)$$

$$\alpha = 1.358M_W + 173.1 \quad (77)$$

$$B = 2.019 \times 10^{-3}e^{-3.193\times10^{-3}M_W} \quad (78)$$

$$L_v = 4.171 \times 10^{-2}e^{-5.119\times10^{-3}M_W} \quad (79)$$

For the alcohol family, the correlations are:

$$m = 0.2348CN + 1.263 \quad (80)$$

$$m\sigma^3 = 25.64CN + 32.22 \quad (81)$$

$$m\varepsilon = 91.37CN + 229.8 \quad (82)$$

$$c = 4.6 \times 10^{-23}{M_W}^2 - 1.82 \times 10^{-21}M_W + 3.78 \times 10^{-20} \quad (83)$$

$$\alpha = 4.059M_W + 40.12 \quad (84)$$

$$B = 0.0058e^{-0.0086M_W} \quad (85)$$

$$L_v = 0.222e^{-0.0123M_W} \quad (86)$$